using Gray's method, with relapse and NRM, respectively, as a competing risk. Acute GVHD was graded by established criteria.[13] Chronic GVHD was evaluated in patients who survived beyond day +100, and was classified as limited or extensive according to the Seattle criteria.[14] A multivariate Cox model was created for grade II–IV acute GVHD, organ stages of acute GVHD, chronic GVHD, OS, NRM and relapse using stepwise selection at a significance level of 5%. Age, conditioning, disease risk, remission state, donor–recipient sex combination and graft source were used as covariates. For chronic GVHD analysis, a history of acute GVHD was included as covariates. Hazard ratios of the *CCR9* genotype were adjusted by these models. In acute GVHD analysis, patients who died before day +30 were censored. Analysis was carried out using STATA (StataCorp. 2007; Stata Statistical Software: Release 10.0. Special Edition. Stata Corporation, College Station, TX, USA). Data analyses were completed as of January 2007 using the most updated database at each institute.

Results

Patient characteristics

Patient characteristics are summarized in Table 1. Ninety-four male patients and 73 female patients, with a median age of 38 years, were included in the study. Our patients were afflicted with various diseases, including myeloid malignancies ($n=106$), lymphoid malignancies ($n=42$) and benign diseases ($n=19$). Disease risk was standard in 97 patients and high in 70 patients. Standard risk included malignancies in the first and second remission, chronic myelogenous leukemia in the chronic phase, myelodysplastic syndrome with refractory anemia with or without ringed sideroblasts and benign diseases. High risk included all others. Ninety-eight patients with malignant disease received transplantation with their disease in remission. The graft source was BM in 130 patients and PBSCs in 37 patients. The conditioning regimen was myeloablative in 147 patients and reduced-intensity conditioning in 20 patients. TBI was used as part of the conditioning in 98 patients. Myeloablative conditioning regimens for malignancy included BU 16 mg/kg + CY 120 mg/kg ($n=32$), CY 120 mg/kg + TBI 12 Gy ($n=9$), CY 120 mg/kg + TBI 10 Gy + another agent of BU 8 mg/kg, cytarabine 8 g/m^2, etoposide 50 mg/kg or melphalan 140 mg/m^2 ($n=62$), BU 8 mg/kg + melphalan 180 mg/m^2 + TBI 10 Gy ($n=12$) and melphalan 180 mg/m^2 + TBI 10 Gy ($n=13$). Reduced-intensity conditioning regimens for malignancy included fludarabine 125 mg/m^2 + melphalan 100–180 mg/m^2 ($n=20$). Conditioning regimens for aplastic anemia included CY 200 mg/kg + TLI 7.5 Gy ($n=17$) and CY 200 mg/kg + TLI 5 Gy + TBI 5 Gy ($n=1$) as previously described.[15] One patient with paroxysmal nocturnal hemoglobinuria was conditioned with CY 120 mg/kg + TBI 12 Gy. At a median follow-up of 42 months (range: 2–220 months), 104 patients were still alive. The estimated 4-year OS, NRM and relapse rates were 55, 18 and 30%, respectively. Causes of 26 non-relapse mortalities included bronchiolitis obliterans ($n=2$), idiopathic pneumonia syndrome ($n=8$), hepatic failure ($n=1$), veno-occlusive

Table 1 Patient characteristics

No. of patients	167
Median age in years (range)	38 (15–62)
Sex (M/F)	94/73
Race (Japanese/other)	167/0
Disease	
AML	50
ALL	30
CML	40
MDS	16
ML	6
ATL	1
MM	5
AA	18
PNH	1
Disease risk	
Standard	97
High	70
Status at transplant among patients with malignant disease	
Remission	98
Non-remission	50
Graft source	
Bone marrow	130
PBSC	37
Gender compatibility	
Female donor in male recipient	45
Others	122
Conditioning	
TBI-containing conditioning	98
Myeloablative conditioning for malignancy	147
BU + CY	32
CY + TBI	9
CY + TBI + another agent	62
BU + melphalan + TBI	12
Melphalan + TBI	13
Reduced-intensity conditioning for malignancy	20
Fludarabine + melphalan	20
Conditioning for aplastic anemia/PNH	
CY + TLI	17
CY + TLI + TBI	1
CY + TBI	1
GVHD prophylaxis	
Cyclosporine + MTX	167
Overall survival at 4 years	55%
Non-relapse mortality at 4 years	18%
Relapse rate at 4 years	30%
Acute GVHD	
Grade (0/I/II/III/IV)	99/37/20/8/3
Skin stage (0/1/2/3/4)	104/33/6/22/2
Liver stage (0/1/2/3/4)	159/3/1/3/1
Gut stage (0/1/2/3/4)	153/4/2/5/3
Chronic GVHD (n = 155 evaluable)	
None	91
Limited/extensive	13/51
Organ (eye/oral/skin/lung/liver)	21/55/31/2/29

Abbreviations: AA = aplastic anemia; ATL = adult T-cell leukemia/lymphoma; F = female; M = male; MDS = myelodysplastic syndrome; ML = malignant lymphoma; MM = multiple myeloma; PNH = paroxysmal nocturnal hemoglobinuria.

Table 2 Proportion of patients who developed GVHD in each genotype

Events	*Genotype 926AG*	*Genotype 926AA*
Acute GVHD		
Grade II–IV	2/10 (20%)	29/157 (18%)
Skin stage 2–4	4/10 (40%)	26/157 (17%)
Liver stage 2–4	1/10 (10%)	4/157 (2.5%)
Gut stage 2–4	1/10 (10%)	9/157 (5.7%)
Chronic GVHD		
Limited/extensive	4/10 (40%)	60/145 (41%)
Eye	2/10 (20%)	19/145 (13%)
Oral	4/10 (40%)	51/145 (35%)
Skin	3/10 (30%)	28/145 (19%)
Lung	1/10 (10%)	1/145 (0.6%)
Liver	2/10 (20%)	27/145 (19%)

disease ($n=2$), hepatitis ($n=2$), intestinal bleeding ($n=1$), transplant-associated microangiopathy ($n=3$), acute GVHD ($n=3$), scleroderma ($n=1$) and bacterial or fungal pneumonia ($n=3$). The incidence rates of grade II–IV, III–IV acute GVHD and chronic limited/extensive GVHD were 18.6, 6.6 and 41%, respectively. The incidence rates of stage 2–4 skin, liver and gut involvement were 18, 3 and 6%, respectively.

Frequency of CCR9 genotypes

Ten donors had genotype 926AG by the RFLP method, which was subsequently confirmed using direct sequence. The frequencies of the 926AA, 926AG and 926GG genotypes among the donors were 94, 6 and 0%, respectively, which were comparable with those reported in the HapMap-JPT database (http://www.hapmap.org).

Hazard analysis and the effect of CCR9 genotypes on transplant outcome

The proportion of patients who developed GVHD in each genotype is summarized in Table 2. Grade II–IV GVHD, stage 2–4 skin GVHD, stage 2–4 liver GVHD, stage 2–4 gut GVHD and chronic limited/extensive GVHD developed in 2, 4, 1, 1 and 4 patients, respectively, among patients whose donor had the genotype 926AG, whereas they developed in 29, 26, 4, 9 and 60 patients, respectively, among patients whose donor had the genotype 926AA. The estimated 4-year OS, NRM and relapse rates were not significantly different between G926A genotypes (56 vs 55%, $P=0.78$; 33 vs 17%, $P=0.32$; 10 vs 32%, $P=0.19$, respectively) (Figure 1). Multivariate analyses showed that PBSC transplantation was a risk factor for grade II–IV GVHD, stage 2–4 skin GVHD and stage 2–4 gut GVHD; high risk disease was a risk factor for OS and relapse; age of more than 40 years was a risk factor for OS and NRM; and female-to-male transplantation was a risk factor for chronic liver GVHD (Table 3, middle column). Hazard ratios of the genotype 926AG, adjusted by these factors, are listed in Table 3 (right column). The genotype 926AG was significantly associated with acute stage 2–4 skin GVHD (hazard ratio: 3.2; 95% confidence interval (95% CI): 1.1–9.1; $P=0.032$) and chronic skin GVHD (hazard ratio: 4.1; 95% CI: 1.1–15; $P=0.036$), whereas it was not

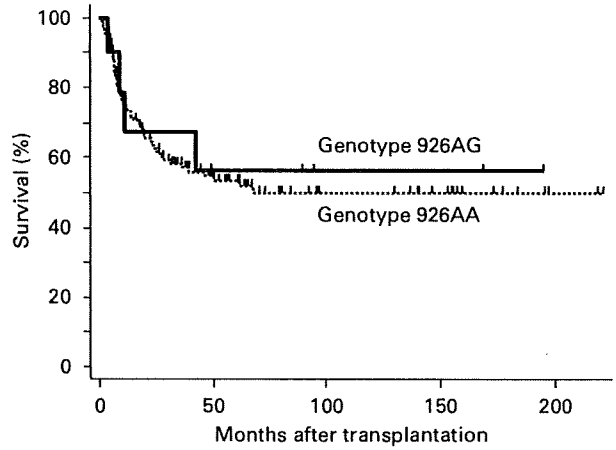

Figure 1 Overall survival between G926A genotypes. At a median follow-up of 42 months (range: 2–220 months), the estimated 4-year overall survival was not statistically different between G926A genotypes (56 vs 55%, $P=0.78$).

associated with grade II–IV GVHD or with stage 2–4 liver GVHD, stage 2–4 gut GVHD, limited or extensive chronic GVHD, chronic GVHD in organs other than skin, OS, NRM or relapse. PBSCs were used in only 1 of 10 patients who received transplantation from 926AG donors.

Functional comparison between CCR9-926A and 926G

To clarify the functional differences between genotypes of 926A and 926G, we created cDNA constructs with each genotype using the Quickchange Kit. Each construct was transfected into Jurkat cells with retroviral vectors. After 3 weeks of selection with puromycin, we analyzed the expression of CCR9 in each of the stably transfected cells. Cells were stained with phycoerythrin-labeled monoclonal anti-CCR9. The level of CCR9 expression was higher in CCR9-transfected cells compared with that in control-transfected cells, and equivalent between the 926A and 926G genotypes (Figure 2a).

We next analyzed the migration of Jurkat cells transfected with control vectors, 926A and 926G, as well as plain Jurkat cells in response to varying concentrations of CCL25, using porous Transwell tissue culture inserts to separate the cells in the upper chambers from the chemokine-containing medium in the lower chambers. As shown in Figure 2b, *CCR9*-transfected cells, but not the control-transfected or plain Jurkat cells, migrated in response to CCL25 in a dose-dependent manner, producing a bell-shaped curve. It is noted that *CCR9*-926G-expressing cells were more responsive to CCL25 compared with those expressing *CCR9*-926A.

Discussion

Several genetic polymorphisms of inflammatory cytokine genes are reported to affect the outcome of allo-HSCT.[16–21] Chemokines are another group of cytokines that control the trafficking of leukocytes through interactions with chemokine receptors. We hope to clarify the role of these

Table 3 Effect of the *CCR9* genotype on transplant outcome

Events	*Risk factor(s)*	*Multivariate*[a]		*Genotype 926AG*[b]	
		Hazard ratio (CI)	P-*value*	*Hazard ratio (CI)*	P-*value*
Acute GVHD					
Grade II–IV	PBSCT	3.4 (1.7–6.9)	0.001	1.2 (0.30–5.3)	0.76
Skin stage 2–4	PBSCT	2.7 (1.3–5.5)	0.008	3.2 (1.1–9.1)	0.032
Liver stage 2–4	—	—	—	4.2 (0.47–37)	0.20
Gut stage 2–4	PBSCT	5.7 (1.6–20)	0.007	2.4 (0.30–19)	0.41
Chronic GVHD					
Limited/extensive	—	—	—	1.7 (0.52–5.8)	0.37
Eye	—	—	—	6.2 (0.56–68)	0.14
Oral	—	—	—	2.4 (0.71–8.4)	0.16
Skin	—	—	—	4.1 (1.1–15)	0.036
Lung	—	—	—	12 (0.76–196)	0.077
Liver	Female to male	3.5 (1.0–12)	0.05	1.7 (0.21–13)	0.63
Overall survival	Age>40	2.1 (1.3–3.6)	0.004	0.84 (0.30–2.3)	0.73
	High risk	2.1 (1.3–3.6)	0.004		
Non-relapse mortality	Age>40	2.7 (1.2–6.1)	0.015	1.3 (0.40–4.5)	0.64
Relapse	High risk	4.0 (2.0–7.8)	<0.001	0.36 (0.05–2.6)	0.31

Abbreviations: CI = confidence interval; PBSCT = peripheral blood stem cell transplantation.
[a]Covariates used were age, conditioning, disease risk, remission state, donor–recipient sex combination and graft source. For chronic GVHD analysis, history of acute GVHD was included in the covariates. Only significant factors were listed.
[b]Adjusted by significant factors.

chemokines in initiating GVHD. Specifically, we address the association of polymorphism in the tissue-specific chemokine receptor gene with acute and chronic GVHD and the regulation of leukocyte trafficking.

CCL25 and CCR9 (as chemokine and chemokine receptor) are selectively expressed in both the thymus and the small intestine.[22,23] One of their important functions is the selective homing and retention of CCR9-positive T cells and B cells to the small intestine rather than to the colon, which provides a mechanism for regional specialization of the mucosal immune system.[9,24] Another function is regulating intrathymic T-cell development, particularly double-negative to double-positive transition,[25,26] which may be associated with T-cell recovery after allo-HSCT. Therefore, the effect of the *CCR9* genotype on acute GVHD is hypothesized to result from its function in the small intestine because T cells educated in the thymus will appear at least 6 months after transplantation.[27]

Interestingly, donor *CCR9* SNPs affected the incidence of skin GVHD, but did not affect the incidence of intestinal GVHD. This observation may be partially explained by the findings of Beilhack *et al.*,[28] who recently reported the redundancy of secondary lymphoid organs at different anatomical sites in GVHD initiation. They suggested that primed T cells could initiate GVHD at sites other than their original priming sites. As Peyer's patches are important sites of Ag presentation,[29] differences in T cell homing to Peyer's patches between each *CCR9* genotype may produce changes in Ag presentation and result in varying incidences of skin GVHD.

Our results suggest the possibility of CCL25/CCR9-targeting modalities for GVHD. CCL25 and CCR9 have an important role in the adherence of T lymphocytes to the intestinal endothelium under inflammatory and normal conditions, and anti-CCL25 Ab attenuates the TNF-α-induced T-cell adhesion in the small intestine.[30] Although blocking the interactions of CCL25 and CCR9 may delay immunological reconstitution in the thymus, CCR9-deficient mice showed no major effect on intrathymic T-cell development despite a 1-day lag in the appearance of double-positive cells and a diminution of γδ-T cells.[31]

One possible limitation of this study is that genetic associations can be biased by population stratification,[32] and there is also the chance of false-positive associations with the *CCR9* genotype on the basis of multiple statistical tests. Confirmation of the results with another separate cohort is needed for eliminating a possible confounding effect. Another limitation is that this SNP might be in linkage disequilibrium with SNPs in the *CCR9* gene or in the other genes located nearby. Linkage disequilibrium mapping of *CCR9* using the HapMap-JPT database showed one small block in introns of the *CCR9* gene, but G926A was outside the block with no known associations with other SNPs in the *CCR9* gene or with genes located around chromosome 3p21.3. In addition, this SNP alters CCR9 amino acid sequences of the third exoloop, which is an important site for chemokine binding and specificity.[33] Therefore, this SNP can affect biological functions due to altered efficiencies of the receptor or signal transduction from the receptor. Although Transwell assays using SNP-transfected cells showed that biological functions varied according to this SNP, the elucidation of additional mechanisms are matters for future research.

In summary, this study suggests that donor 926AG is associated with an increased incidence of acute and chronic skin GVHD in related HSCT recipients. CCL25 and CCR9

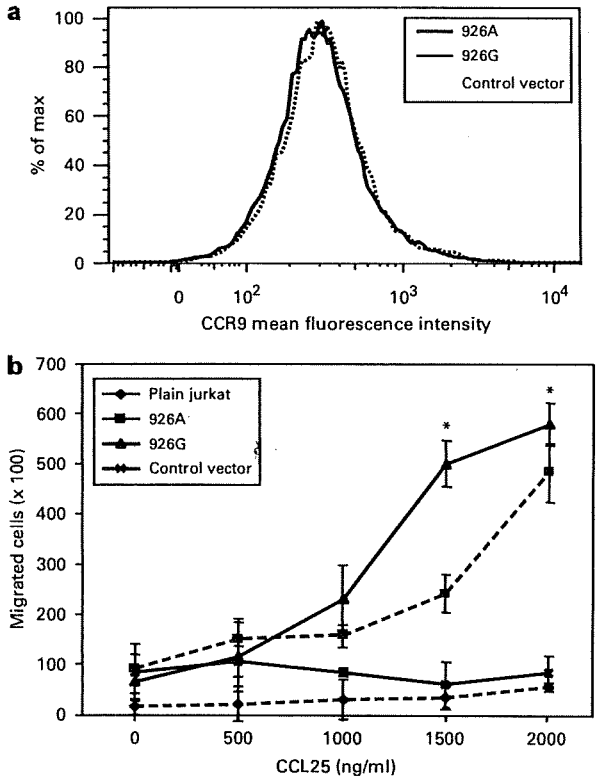

Figure 2 Chemotaxis assays with *CCR9*-polymorphism-transfected Jurkat cells: (a) Flow cytometric analysis of CCR9 expression. Transfected Jurkat cells were stained with phycoerythrin (PE)-labeled monoclonal anti-CCR9. Control staining with control-transfected Jurkat cells is also shown (shadow); (b) Jurkat cells transfected with cDNAs encoding *CCR9* migrated in response to CCL25. After puromycin selection, 1×10^6 transfected cells and the same number of Jurkat cells were added to porous Transwell tissue culture inserts and placed in wells containing various concentrations of CCL25. After 90-min of incubation, cells migrating through the membranes into the lower wells were counted. Results are expressed as cells migrating per 10^6 input cells. Assays were carried out in triplicate and error bars represent s.d. $^*P<0.05$

may be candidates for future therapeutic targets that alter the quality and incidence of GVHD.

Conflict of interest

The authors declare no conflict of interest.

Acknowledgements

We thank Dr Toshio Kitamura for providing the pMX-IRES-Puro vector and PLAT-A packaging cells. This study was supported in part by a Health and Labor Science Research Grant (20251001) from the Ministry of Health, Labour and Welfare of Japan, a Grant-in-Aid for Scientific Research (20591149 and 19591105) from the Ministry of Education, Culture, Sports, Science and Technology, and Grants-in-Aid from the National Institute of Biomedical Innovation and the Sankyo Memorial Foundation, Japan.

References

1 Perfetti P, Carlier P, Strada P, Gualandi F, Occhini D, Van Lint MT *et al.* Extracorporeal photopheresis for the treatment of steroid refractory acute GVHD. *Bone Marrow Transplant* 2008; **42**: 609–617.
2 Kunkel EJ, Butcher EC. Chemokines and the tissue-specific migration of lymphocytes. *Immunity* 2002; **16**: 1–4.
3 Campbell DJ, Kim CH, Butcher EC. Chemokines in the systemic organization of immunity. *Immunol Rev* 2003; **195**: 58–71.
4 Campbell JJ, Butcher EC. Chemokines in tissue-specific and microenvironment-specific lymphocyte homing. *Curr Opin Immunol* 2000; **12**: 336–341.
5 Moser B, Loetscher P. Lymphocyte traffic control by chemokines. *Nat Immunol* 2001; **2**: 123–128.
6 Pan J, Kunkel EJ, Gosslar U, Lazarus N, Langdon P, Broadwell K *et al.* A novel chemokine ligand for CCR10 and CCR3 expressed by epithelial cells in mucosal tissues. *J Immunol* 2000; **165**: 2943–2949.
7 Wang W, Soto H, Oldham ER, Buchanan ME, Homey B, Catron D *et al.* Identification of a novel chemokine (CCL28), which binds CCR10 (GPR2). *J Biol Chem* 2000; **275**: 22313–22323.
8 Kunkel EJ, Campbell JJ, Haraldsen G, Pan J, Boisvert J, Roberts AI *et al.* Lymphocyte CC chemokine receptor 9 and epithelial thymus-expressed chemokine (TECK) expression distinguish the small intestinal immune compartment: epithelial expression of tissue-specific chemokines as an organizing principle in regional immunity. *J Exp Med* 2000; **192**: 761–768.
9 Papadakis KA, Prehn J, Nelson V, Cheng L, Binder SW, Ponath PD *et al.* The role of thymus-expressed chemokine and its receptor CCR9 on lymphocytes in the regional specialization of the mucosal immune system. *J Immunol* 2000; **165**: 5069–5076.
10 Stenstad H, Svensson M, Cucak H, Kotarsky K, Agace WW. Differential homing mechanisms regulate regionalized effector CD8alphabeta+ T cell accumulation within the small intestine. *Proc Natl Acad Sci U S A* 2007; **104**: 10122–10127.
11 Onishi M, Kinoshita S, Morikawa Y, Shibuya A, Phillips J, Lanier LL *et al.* Applications of retrovirus-mediated expression cloning. *Exp Hematol* 1996; **24**: 324–329.
12 Yu CR, Peden KW, Zaitseva MB, Golding H, Farber JM. CCR9A and CCR9B: two receptors for the chemokine CCL25/TECK/Ck beta-15 that differ in their sensitivities to ligand. *J Immunol* 2000; **164**: 1293–1305.
13 Przepiorka D, Weisdorf D, Martin P, Klingemann HG, Beatty P, Hows J *et al.* 1994 Consensus Conference on Acute GVHD Grading. *Bone Marrow Transplant* 1995; **15**: 825–828.
14 Sullivan KM, Agura E, Anasetti C, Appelbaum F, Badger C, Bearman S *et al.* Chronic graft-versus-host disease and other late complications of bone marrow transplantation. *Semin Hematol* 1991; **28**: 250–259.
15 Inamoto Y, Suzuki R, Kuwatsuka Y, Yasuda T, Takahashi T, Tsujimura A *et al.* Long-term outcome after bone marrow transplantation for aplastic anemia using cyclophosphamide and total lymphoid irradiation as conditioning regimen. *Biol Blood Marrow Transplant* 2008; **14**: 43–49.
16 Kallianpur AR. Genomic screening and complications of hematopoietic stem cell transplantation: has the time come? *Bone Marrow Transplant* 2005; **35**: 1–16.
17 Dickinson AM, Middleton PG, Rocha V, Gluckman E, Holler E. Genetic polymorphisms predicting the outcome of bone marrow transplants. *Br J Haematol* 2004; **127**: 479–490.
18 Lin MT, Storer B, Martin PJ, Tseng LH, Gooley T, Chen PJ *et al.* Relation of an interleukin-10 promoter polymorphism to graft-versus-host disease and survival after hematopoietić-cell transplantation. *N Engl J Med* 2003; **349**: 2201–2210.

19 Socie G, Loiseau P, Tamouza R, Janin A, Busson M, Gluckman E *et al.* Both genetic and clinical factors predict the development of graft-versus-host disease after allogeneic hematopoietic stem cell transplantation. *Transplantation* 2001; **72**: 699–706.
20 Cavet J, Dickinson AM, Norden J, Taylor PR, Jackson GH, Middleton PG. Interferon-gamma and interleukin-6 gene polymorphisms associate with graft-versus-host disease in HLA-matched sibling bone marrow transplantation. *Blood* 2001; **98**: 1594–1600.
21 Mehta PA, Eapen M, Klein JP, Gandham S, Elliott J, Zamzow T *et al.* Interleukin-1 alpha genotype and outcome of unrelated donor haematopoietic stem cell transplantation for chronic myeloid leukaemia. *Br J Haematol* 2007; **137**: 152–157.
22 Zaballos A, Gutierrez J, Varona R, Ardavin C, Marquez G. Cutting edge: identification of the orphan chemokine receptor GPR-9-6 as CCR9, the receptor for the chemokine TECK. *J Immunol* 1999; **162**: 5671–5675.
23 Zabel BA, Agace WW, Campbell JJ, Heath HM, Parent D, Roberts AI *et al.* Human G protein-coupled receptor GPR-9-6/CC chemokine receptor 9 is selectively expressed on intestinal homing T lymphocytes, mucosal lymphocytes, and thymocytes and is required for thymus-expressed chemokine-mediated chemotaxis. *J Exp Med* 1999; **190**: 1241–1256.
24 Mora JR, von Andrian UH. Role of retinoic acid in the imprinting of gut-homing IgA-secreting cells. *Semin Immunol* 2009; **21**: 28–35.
25 Wurbel MA, Philippe JM, Nguyen C, Victorero G, Freeman T, Wooding P *et al.* The chemokine TECK is expressed by thymic and intestinal epithelial cells and attracts double- and single-positive thymocytes expressing the TECK receptor CCR9. *Eur J Immunol* 2000; **30**: 262–271.
26 Norment AM, Bogatzki LY, Gantner BN, Bevan MJ. Murine CCR9, a chemokine receptor for thymus-expressed chemokine that is up-regulated following pre-TCR signaling. *J Immunol* 2000; **164**: 639–648.
27 Heitger A, Neu N, Kern H, Panzer-Grumayer ER, Greinix H, Nachbaur D *et al.* Essential role of the thymus to reconstitute naive (CD45RA+) T-helper cells after human allogeneic bone marrow transplantation. *Blood* 1997; **90**: 850–857.
28 Beilhack A, Schulz S, Baker J, Beilhack GF, Nishimura R, Baker EM *et al.* Prevention of acute graft-versus-host disease by blocking T-cell entry to secondary lymphoid organs. *Blood* 2008; **111**: 2919–2928.
29 Niess JH, Reinecker HC. Lamina propria dendritic cells in the physiology and pathology of the gastrointestinal tract. *Curr Opin Gastroenterol* 2005; **21**: 687–691.
30 Hosoe N, Miura S, Watanabe C, Tsuzuki Y, Hokari R, Oyama T *et al.* Demonstration of functional role of TECK/CCL25 in T lymphocyte-endothelium interaction in inflamed and uninflamed intestinal mucosa. *Am J Physiol Gastrointest Liver Physiol* 2004; **286**: G458–G466.
31 Wurbel MA, Malissen M, Guy-Grand D, Meffre E, Nussenzweig MC, Richelme M *et al.* Mice lacking the CCR9 CC-chemokine receptor show a mild impairment of early T- and B-cell development and a reduction in T-cell receptor gammadelta(+) gut intraepithelial lymphocytes. *Blood* 2001; **98**: 2626–2632.
32 Wacholder S, Rothman N, Caporaso N. Counterpoint: bias from population stratification is not a major threat to the validity of conclusions from epidemiological studies of common polymorphisms and cancer. *Cancer Epidemiol Biomarkers Prev* 2002; **11**: 513–520.
33 Youn·BS, Yu KY, Oh J, Lee J, Lee TH, Broxmeyer HE. Role of the CC chemokine receptor 9/TECK interaction in apoptosis. *Apoptosis* 2002; **7**: 271–276.

Cancer Science
The official journal of the Japanese Cancer Association

Irrespective of CD34 expression, lineage-committed cell fraction reconstitutes and re-establishes transformed Philadelphia chromosome-positive leukemia in NOD / SCID / IL-2Rγc$^{-/-}$ mice

Ryohei Tanizaki,[1,6] Yuka Nomura,[1,6] Yasuhiko Miyata,[1] Yosuke Minami,[1] Akihiro Abe,[1] Akitoshi Hanamura,[2] Masashi Sawa,[3] Makoto Murata,[1] Hitoshi Kiyoi,[4] Tadashi Matsushita[1] and Tomoki Naoe[1,5]

[1]Department of Hematology and Oncology, Nagoya University Graduate School of Medicine, Nagoya; [2]Department of Hematology, Gifu Prefectural Tajimi Hospital, Tajimi; [3]Department of Hematology, Anjo Kosei Hospital, Anjo; [4]Department of Infectious Diseases, Nagoya University Hospital, Nagoya, Japan

(Received August 31, 2009/Revised October 21, 2009/Accepted November 03, 2009/Online publication December 18, 2009)

Stem cells of acute myeloid leukemia (AML) have been identified as immunodeficient mouse-repopulating cells with a Lin$^-$CD34$^+$38$^-$ phenotype similar to normal hematopoietic stem cells. To identify the leukemia-propagating stem cell fraction of Philadelphia chromosome-positive (Ph$^+$) leukemia, we serially transplanted human leukemia cells from patients with chronic myeloid leukemia blast crisis (n = 3) or Ph$^+$ acute lymphoblastic leukemia (n = 3) into NOD/SCID/IL-2Rγc$^{-/-}$ mice. Engrafted cells were almost identical to the original leukemia cells as to phenotypes, *IGH* rearrangements, and karyotypes. CD34$^+$CD38$^-$CD19$^+$, CD34$^+$38$^+$CD19$^+$, and CD34$^-$CD38$^+$ CD19$^+$ fractions could self-renew and transfer the leukemia, whereas the CD34$^-$CD38$^+$CD19$^+$ fraction did not stably propagate in NOD/SCID mice. These findings suggest that leukemia-repopulating cells in transformed Ph$^+$ leukemia are included in a lineage-committed but multilayered fraction, and that CD34$^+$ leukemia cells potentially emerge from CD34$^-$ populations. (*Cancer Sci* 2010; 101: 631–638)

The current concept of leukemia stem cells (LSCs) has significantly influenced the view of the development and treatment of leukemia.[1–5] Intravenous injection of human leukemia cells into NOD/SCID mice, which is now a common and reliable method to identify human hematopoietic stem cells (HSCs) *in vivo*, shows that leukemia cells expressing primitive cell surface makers such as Lin$^-$CD34$^+$CD38$^-$ can repopulate NOD/SCID mice regardless of the type of acute myeloid leukemia (AML).[1,6–9] Serial transplantation of only this fraction can propagate AML from mouse to mouse. AML LSCs have a hierarchy similar to normal HSCs and also show other characteristics of HSCs such as quiescence, chemotherapy-resistance, and osteoblastic niche-dependence.[9,10] However, there are limited but conflicting data about LSCs in acute lymphoblastic leukemia (ALL).[11–19] For example, it remains unclear whether ALL LSCs have a stem cell phenotype. Chronic myelogenous leukemia (CML) has been thought to be a stem cell disease, because the Philadelphia chromosome (Ph) can be detected in not only all myeloid cells but also in some lymphoid cells.[20] In addition, *BCR-ABL* mRNA is detected in the patients' HSC fraction (Lin$^-$CD34$^+$CD38$^-$CD90$^+$).[21] In CML blast crisis (CML-BC), progenitor cells have been shown to acquire self-renewal capacity through additional gene alterations,[21,22] however, it remains unclear whether LSCs in CML-BC are phenotypically different from AML or ALL, and how leukemia cells are hierarchically controlled. Furthermore, the difference between leukemia stem cells in Ph$^+$ ALL and CML-BC remains unknown. To address these questions, we used NOD/SCID/IL-2Rγc$^{-/-}$ (NOG) mice, which are more severely immunocompromised than NOD/SCID mice, and therefore permit increased engraftment of human cells and present a more sensitive mouse model for detecting human HSCs and LSCs.[10,23] In this system, we found that engrafted cells were lineage-committed and clonal in the *IGH* gene rearrangements, irrespective of stem/progenitor cell markers. Lineage-committed fractions, including CD34$^+$CD38$^+$ and CD34$^-$CD38$^+$ fractions, could self-renew and transfer leukemia in mice, indicating that leukemia-repopulating cells in Ph$^+$ leukemia are multilayered but phenotypically different from normal HSCs. *Ex vivo* culture of Ph$^+$ leukemia cells showed a similar maturation course based on surface makers. However, transplantation of the CD34$^-$CD38$^+$ fraction gave rise to immature populations, such as the CD34$^+$CD38$^+$ and CD34$^+$CD38$^-$ fractions, in NOG mice, suggesting that the CD34 expression of human leukemia cells is potentially reversible *in vivo*.

Materials and Methods

Patients. The patients' characteristics are shown in Table 1. CML-BC or Ph$^+$ ALL was diagnosed according to hematological findings, the clinical course, chromosomal analyses, and cell phenotypes. Samples from unique patient number (UPN)2, UPN3, and UPN4 and those from UPN1, UPN5, and UPN6 were obtained at diagnosis and at relapse after imatinib-containing therapy, respectively. Primary leukemia cells from patient bone marrow (BM) were collected after obtaining written informed consent. Each sample contained more than 80% of leukemia cells.

Flow cytometry analysis and cell sorting. Bone marrow mononuclear cells were separated by Ficoll-Paque PLUS (Amersham Biosciences, Uppsala, Sweden) density-gradient centrifugation and suspended in PBS with 2% FBS (Gibco BRL, Carlsbad, CA, USA). Mononuclear cells were stained with lineage-associated phycoerythrin (PE)-Cy5.5-conjugated antibodies, including CD2, CD3, CD4, CD8, CD14, CD19, CD20, and CD56 from Caltag Laboratories (Burlingame, CA, USA), except the markers positive in leukemia cells. Cells with lineage cocktail antibodies were further incubated with HSC-associated antibodies consisting of allophycocyanin (APC)-conjugated anti-CD34 (HPCA-2; Becton Dickinson PharMingen, Franklin Lakes, NJ, USA), PE-Cy7-conjugated anti-CD38 (Becton Dickinson PharMingen), FITC-labeled CD47 and PE-conjugated anti-CD90, or with progenitor-associated antibodies consisting of APC-conjugated anti-CD34, PE-Cy7-conjugated anti-CD38, PE-conjugated

[5]To whom correspondence should be addressed.
E-mail: tnaoe@med.nagoya-u.ac.jp
[6]These authors contributed equally to this work.

doi: 10.1111/j.1349-7006.2009.01440.x

Table 1. Comparison of cell markers and karyotypes between original and engrafted leukemia cells

Patient (age/gender, type of leukemia, ABL mutation)	UPN1 (31/F, CML-BC, T315I)		UPN2 (67/M, CML-BC, F311I)		UPN3 (52/F, CML-BC, wild)		UPN4 (77/M, Ph+ ALL, wild)		UPN5 (68/F, Ph+ ALL, wild)		UPN6 (77/F, Ph+ ALL, Y253H)	
	Original	INH (engrafted)	Original	MKS (engrafted)	Original	MIZ (engrafted)	Original	SGR (engrafted)	Original	OMR (engrafted)	Original	KWI (engrafted)
Engraftment efficiency	10×10^6	5/5	4.0×10^6	3/3	4.0×10^6	3/3	10×10^6	3/3	2.5×10^6	4/4	1.5×10^6	5/5
CD2	–	–	–	–	–	–	–	–	–	–	–	ND
CD3	–	–	–	–	–	–	–	–	+/–	Low	–	–
CD4	–	–	–	–	–	–	–	–	–	–	–	–
CD5	–	–	–	–	–	–	–	–	–	–	–	–
CD7	–	–	Low	+/–	–	–	–	–	–	–	–	–
CD10	+	+/–	–	+/–	+	+	+	+	+	+/–	+	+
CD13	–	–	+	+	–	+/–	Low	–	+/–	Low	Low	–
CD14	Low	–	–	–	+/–	–	–	–	–	–	–	–
CD19	+	+	–	–	+	+	+	+	+	+	+	+
cyCD22	ND	+	ND	–	ND	+/–	ND	Low	Low	Low	ND	ND
CD33	–	+/–	+/–	Low	Low	Low	–	+/–	+/–	+/–	Low	–
CD34	+/–	+/–	+	+	+/–	+/–	+	+/–	+	+	+/–	–
CD79a	ND	+	ND	+/–	ND	+/–	ND	+	+	+	ND	ND
MPO	ND	Low	ND	+/–	ND	Low	ND	–	–	–	ND	ND
Karyotype	47,XX, t(9;22) (q34;q11), +mar	ND	46,XY, t(9;22) (q34;q11)	46,XY,del(1) (p13p22), add(5), t(9,22) (q34;q11)	46,XX, t(9;22) (q34;q11)	44,X,-X or-Y, -6.-10.-12,-18, -21,-22,+4mar 46,X,-X or -Y,-9, -10,-17,;3mar	45,XY, der(7:12) (q10;q10), t(9:22) (q34;q11)	45,XY,der(7;12) (q10;q10), t(9;22) (q34+q11.2), -10,mar	46,XX, t(9;22) (q34;q11) 45,XX,idem dic(8;12) (p11;p11)	46,XX,t(9;22) (q34;q11.2)	46,XX -2,-7,t(9;22) (q34;q11.2), +2mar	46,XX,t(2;7) (p11.2;p13), t(9;22) (q34;q11.2)

Original and engrafted leukemia cells were analyzed for surface markers, gene mutations at the kinase domain of the BCR-ABL, and karyotypes. The number of original cells transplanted into NOD/SCID/IL-2Rγc$^{-/-}$ mice and engraft-efficiency are described. +, positive; –, negative, +/–, positive/negative. ALL, acute lymphoblastic leukemia; CML-BC, Chronic myelogenous leukemia blast crisis; cy, cytoplasmic; MPO, myeloperoxidase; ND, not done; Ph+, Philadelphia chromosome-positive.

doi: 10.1111/j.1349-7006.2009.01440.x

anti-interleukin-3 receptor (IL-3R) (9F5; Becton Dickinson PharMingen), and FITC-conjugated anti-CD45RA (MEM56; Caltag Laboratories).

Flow cytometry analysis and cell sorting were carried out as previously reported.[21,22,24] After staining, cells were analyzed and sorted using a modified FACSAria (Becton Dickinson Immunocytometry Systems, Franklin Lakes, NJ, USA) equipped with a 488-nm argon laser and a 633-nm He-Ne laser and FlowJo software (Tree Star, San Carlos, CA, USA). Lin^-CD34^+ cells were divided into HSCs ($Lin^-CD34^+CD38^-$) and progenitors ($Lin^-CD34^+CD38^+$). HSCs were further separated into long-term HSCs ($Lin^-CD34^+CD47^+CD90^+$) and short-term HSCs ($Lin^-CD34^+CD47^+CD90^-$). Progenitors were further separated into common myeloid progenitors ($Lin^-CD34^+CD38^+IL\text{-}3R^+CD45RA^-$) and their progeny, including granulocyte/monocyte progenitor (GMP; $Lin^-CD34^+CD38^+IL\text{-}3R^+CD45RA^+$), and megakaryocyte/erythroid progenitors ($Lin^-CD34^+CD38^+IL\text{-}3R^-CD45RA^-$).

Xenotransplantation into NOG mice. NOG and NOD/SCID mice were obtained from the Central Institute for Experimental Animals (Kawasaki, Japan) and Clea Japan (Tokyo, Japan), respectively. Human leukemia cells ($1.5–10 \times 10^6$ cells) were injected into the tail vein of non-irradiated 8-week-old male NOG mice. To prevent human T cell expansion, 0.1 mg anti-CD3 antibody (Janssen Pharmaceutical, Tokyo, Japan) was injected on the same day, as described previously.[10] For the *in vivo* passage of leukemia cells, BM cells or spleen cells ($1–5 \times 10^6$ cells) from a NOG mouse were injected into another NOG mouse with an 8- to 16-week interval. To analyze the repopulating activity in mice, $5–10 \times 10^3$ fractionated leukemia cells were serially transplanted together with 0.1×10^6 mouse BM cells. Pathological examination was done as described.[10] The animal experiments were approved by the institutional ethics committee for Laboratory Animal Research, Nagoya University School of Medicine (Nagoya, Japan) and carried out according to the guidelines of the institute.

Mutation analysis of the *ABL* kinase domain. RNA was isolated from BM mononuclear cells by RNA STAT-60TM (Tel-Test, Friendswood, TX, USA) and cDNA synthesized by reverse transcriptase (TaqMan Gold RT-PCR Kit; Applied Biosystems, Foster City, CA, USA). The kinase domain of *BCR-ABL* was sequenced following the nested PCR method. BCR-ABL was first amplified for 35 cycles (94°C for 30 sec, 60°C for 30 sec, 72°C for 3 min) followed by two primers, BCR-2682F (5′-TCCGCTGACCATCAATAAGGA-3′) and ABL-1745R (5′-CTCCGGGGGACCTCGCTCTTT-3′). The amplified fragment was subjected to nested PCR for 30 cycles (94°C for 30 s, 60°C for 30 s, 72°C for 2 min) with primers ABL-772F (5′-GAGGGCGTGTGGAAGAAATA-3′) and ABL-1616R (5′-GCAGCTCTCCTGGAGGTCCTCG-3′). After purification of PCR products using the GeneClean III Kit (Qbiogene, Vista, CA, USA), standard dideoxy chain-termination DNA sequencing was carried out using a BigDye Terminator Cycle Sequencing Kit (Applied Biosystems) on an automated ABI3700 analyzer and analyzed with an ABI PRISM 310 Genetic Analyzer (Applied Biosystems). All mutations were confirmed by sequencing forward and reverse strands.

Southern blot analysis and cloning of IGH complementarity-determining region-3 (CDR-3). High molecular weight DNA was extracted from samples. Southern blot analysis using the *JH* probe was carried out as previously described.[25]

***Ex vivo* culture of human leukemia cells.** Cells were resuspended and cultured in QBSF-60 serum-free media (Quality Biological, Gaithersburg, MD, USA) containing 10 ng/mL recombinant human thrombopoietin (rhTPO), recombinant human stem cell factor (rhSCF), recombinant human FLT3 ligand (rhFLT3L), and 10 ng/mL recombinant human interleukin-7 (rhIL-7). rhTPO and rhSCF were kindly provided by Kirin (Tokyo, Japan). rhFLT3L and rhIL-7 were purchased from PeproTech (Rocky Hill, NJ, USA).

Results

Xenotransplantation of human leukemia cells into NOG mice. We injected unsorted human leukemia cells ($1.5–10 \times 10^6$ cells/mouse) from six patients with CML-BC ($n = 3$) or Ph^+ ALL ($n = 3$) into three to five NOG mice per patient, and observed their engraftment in all mice injected (Table 1). The engraftment of human leukemia cells was confirmed by more than 1% of human $CD45^+$ peripheral blood cells at week 8, and the BM or spleen cells were analyzed and passed intravenously until week 16. Cell markers, karyotypes, and gene mutations at the kinase domain of *BCR-ABL* were almost the same as the original samples (Table 1). In the MIZ line, the karyotype became complex whereas *BCR-ABL* was detected by RT-PCR (data not shown). These six leukemia lines, serially passed *in vivo*, have been propagated for more than 1 year, but were unable to stably proliferate *ex vivo* in culture.

Analysis of HSC and progenitor phenotypes of transplanted leukemia cells. To study the differentiation hierarchy, lineage and stem/progenitor markers were compared between the original and engrafted cells. As shown in Figure 1(a), the CD34/CD38 patterns were almost the same in each experiment. In CML-BC, the major fraction was $CD34^+CD38^+IL\text{-}3R^+CD45RA^+$, indicative of the GMP phenotype. There were minor fractions of $CD34^+CD38^-$ or $CD34^-CD38^+$. In Ph^+ ALL, the phenotype of the OMR line was similar to those of CML-BC lines. The SGR line showed a relatively homogeneous phenotype with regards to CD34/CD38 expression. The KWI line phenotype was shifted to $CD34^-CD38^+$ compared with the original leukemia cells. All leukemia cells, irrespective of CD34 and CD38 expression, expressed lineage markers; CD19 in the INH, MIZ, SGR, OMR, and KWI lines, and CD13 in the MKS line. These data indicate that NOG mice transplanted with leukemia cells can recapture a similar differentiation pattern.

***BCR-ABL* fusion transcripts and mutations at the *ABL* kinase domain.** The major type of *BCR-ABL* fusion transcripts was detected in the original cells and the established INH, MKS, MIZ, and KWI lines. The minor type of transcripts was detected in SGR and OMR. *ABL* kinase domain mutations T315I, F311I, and Y253H were detected in the INH, MKS, and KWI lines and their original cells, respectively (Table 1).

Serial passages of INH and OMR leukemia cells sorted according to CD34 expression. Both $CD34^+$ and $CD34^-$ populations were maintained in the INH and OMR lines. To study which fraction could repopulate leukemia into NOG mice, we transplanted 5×10^3 or 10^4 leukemia cells sorted based on CD34/CD38 expression. The purity of sorted cells was over 98% (Fig. S1). In the INH line, $CD34^+CD38^-$, $CD34^+CD38^+$, and $CD34^-CD38^+$ cells repopulated human leukemia 8 weeks after transplantation ($n = 3$; Fig. 2a). Serial transplantation of 1×10^4 $CD34^-CD38^+$ cells mainly generated $CD34^-CD38^+$ leukemia in the BM; however, $CD34^+CD38^+$ cells faintly emerged in the spleen and BM (Fig. 2a).

In the OMR line, injection of $CD34^-CD38^+$ cells generated all the three factions: $CD34^+CD38^-$, $CD34^+CD38^+$ and $CD34^-CD38^+$ ($n = 3$; Fig. 2b). To further confirm whether $CD34^-$ fresh leukemia cells generated $CD34^+$ cells, we transplanted 2.5×10^4 of $CD34^+$ or $CD34^-$ cells of UPN6 sample into NOG mice ($n = 3$ and $n = 3$, respectively). BM cells showed almost the same pattern of CD34/CD38 expression. Although the main population was $CD34^-CD38^+$, a small population of $CD34^+CD38^+$ was also detected (Fig. 2c). These findings suggest that either $CD34^+CD38^-$, $CD34^+38^+$, or $CD34^-CD38^+$ fractions self-renewed and transferred leukemia

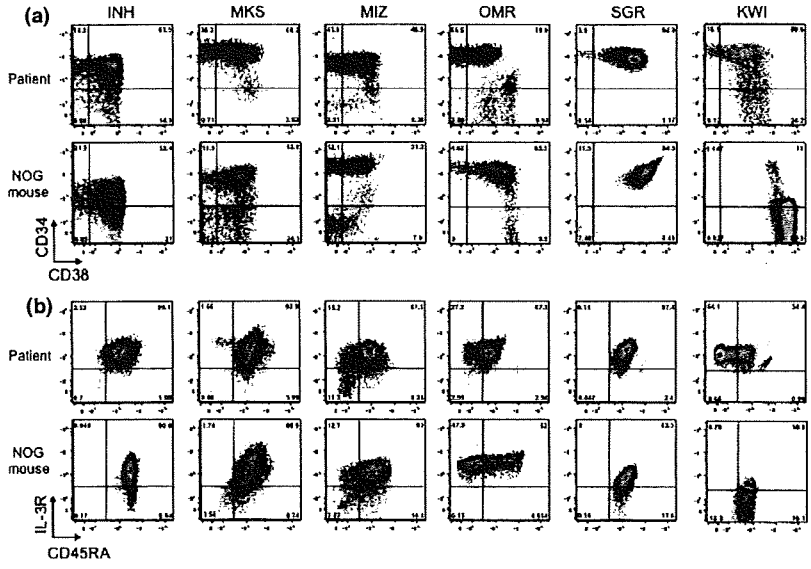

Fig. 1. Bone marrow cells of leukemia-transplanted NOD/SCID/IL-2Rγc$^{-/-}$ (NOG) mice showed a similar human hematopoietic stem cell/progenitor profile to the original patient's bone marrow. (a) CD34/CD38 pattern. (b) Interleukin-3R (IL-3R)/CD45RA pattern in a CD34$^+$CD38$^+$ fraction. Human hematopoietic stem cell/progenitor profiles, which were analyzed by FACSAria and FlowJo software, showed that the percentage of granulocyte/monocyte progenitor fraction is increased.

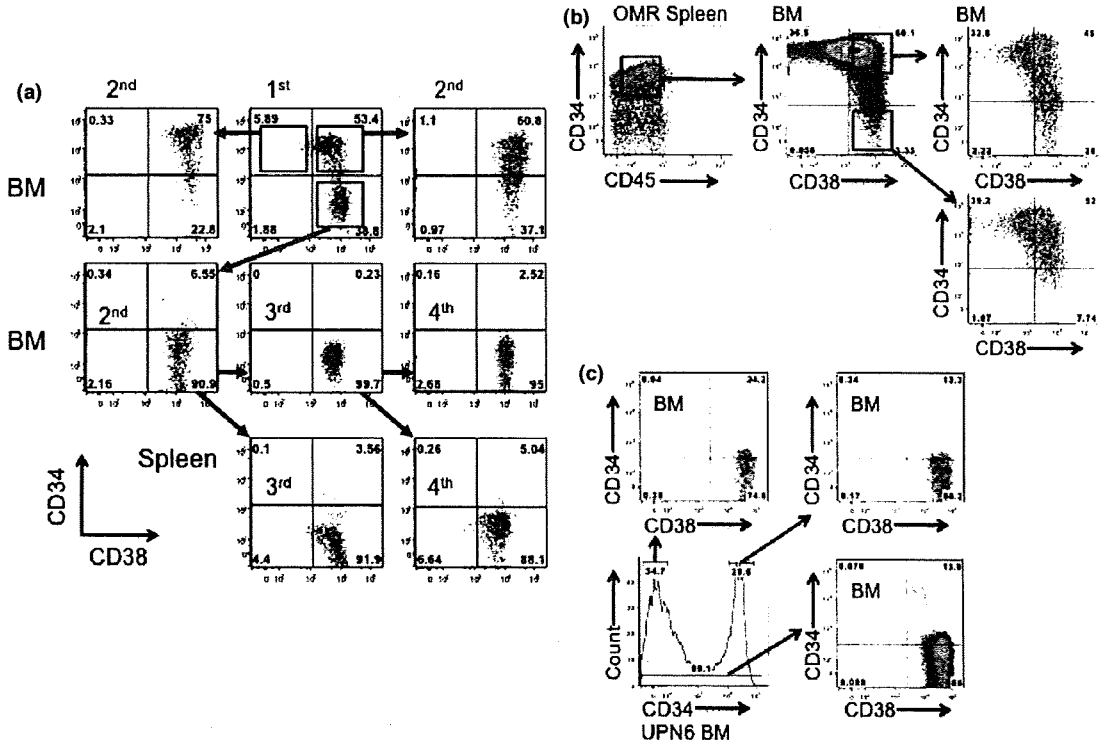

Fig. 2. Both the CD34$^+$ and CD34$^-$ populations of chronic myelogenous leukemia blast crisis (INH) and Philadelphia chromosome-positive acute lymphoblastic leukemia (OMR) cells from primary recipient mouse bone marrow (BM) developed disease. (a) INH cells from a primary recipient mouse of UPN1 were sorted into CD34$^+$CD38$^-$, CD34$^+$CD38$^+$, and CD34$^-$CD38$^+$ fractions. Sorted cells (5×10^3 to 1×10^4) were transplanted into the secondary NOD/SCID/IL-2Rγc$^{-/-}$ (NOG) mice. Tertiary and quaternary transplantations using the CD34$^-$CD38$^+$ population were carried out and CD34/CD38 profiles of leukemia cells from the BM and spleen are shown. (b) OMR cells from the primary recipient mouse spleen of UPN5 were sorted into CD34$^+$CD38$^+$ and CD34$^-$CD38$^+$ fractions and 5×10^4 sorted cells were transplanted into NOG mice. Tertiary transplantation was also carried out. The CD34/CD38 pattern was almost the same between mice transplanted with CD34$^+$CD38$^+$ and CD34$^-$CD38$^+$ BM cells. (c) CD34$^+$ (n = 3) or CD34$^-$ (n = 2) BM cells, or total BM cells (n = 2) (all at 2.5×10^5) from UPN6 were transplanted into NOG mice.

in NOG mice, which does not correspond with previous reports in AML.

To study the possibility that the difference came from using NOG mice, we transplanted CD34/CD38-sorted fractions into NOD/SCID mice. CD34$^+$CD38$^+$ and CD34$^-$CD38$^+$ fractions passed from the CD34$^+$CD38$^+$ fraction of the INH line [(1) and (2) in Fig. 3a] engrafted in NOD/SCID mice as efficiently as in NOG mice (Fig. 2b). The CD34/CD38 pattern was the same as in NOG mice (Fig. 2b). However, the CD34$^+$CD38$^+$ and CD34$^-$CD38$^+$ fractions of INH cells passed from the

doi: 10.1111/j.1349-7006.2009.01440.x

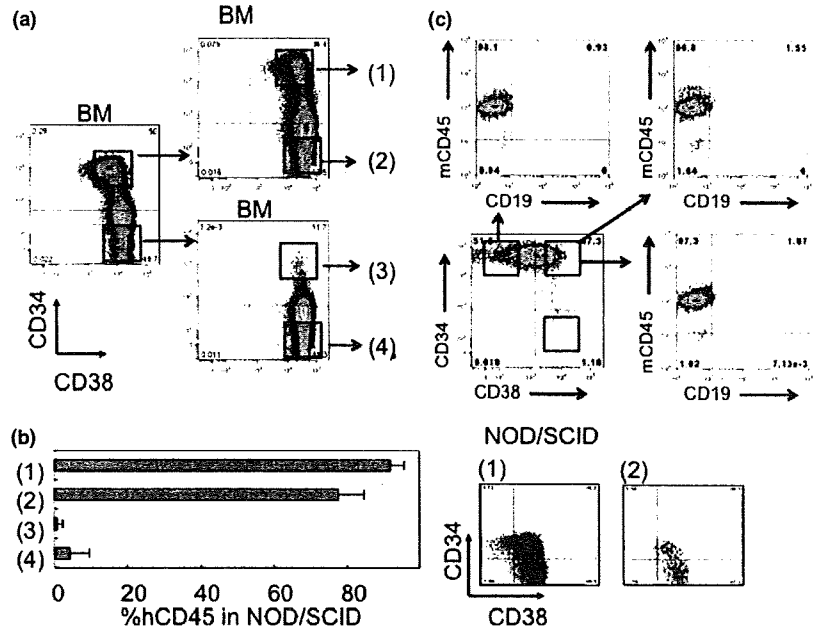

Fig. 3. Human leukemia cells transplanted into NOD/SCID/IL-2Rγc$^{-/-}$ (NOG) mice were not efficiently transferred into NOD/SCID mice. (a) Chronic myelogenous leukemia blast crisis (INH) cells repopulated in NOG mouse bone marrow (BM) were sorted into CD34$^+$CD38$^+$ and CD34$^-$CD38$^+$ fractions and these sorted cells were secondarily transplanted into NOG mice. Cells from the secondary recipient mice BM were further separated according to CD34 expression and 10^4 cells were transplanted into NOD/SCID mice. (b) Chimerism of human CD45$^+$ (hCD45) leukemia cells in NOD/SCID BM was measured by flow cytometry 8 weeks after transplantation (n = 3; left panel). CD34/CD38 expression profiles of fractions (1) and (2)-transplanted NOD/SCID mouse BM are shown (right panel). (c) Fractionated 10^4 OMR cells from NOG mouse BM were transplanted into NOD/SCID mice (n = 3). mCD45, murine CD45.

CD34$^-$CD38$^+$ fraction [(3) and (4) in Fig. 3a] had reduced engraftment in NOD/SCID mice [(3) and (4) in Fig. 3b]. Neither fraction of 1×10^5 OMR cells from NOG mouse BM was transplantable into NOD/SCID mice (Fig. 3c), although it was stably transferred into NOG mice (Fig. 2b). These findings suggest that mouse immunocompetence significantly affects the repopulating activity of leukemia cells, and that the expression of CD34 might be reversible *in vivo*.

***Ex vivo* cell culture.** Each leukemia line was cultured in medium supplemented with FCS and/or an appropriate cytokine cocktail; however, no lines were able to be maintained for more than 2 weeks in culture. INH cells were cultured for 8 days and injected into NOG mice. Although more than 30% of cells were positive for CD34$^+$ after 8 days, the cultured INH cells did not engraft in NOG mice (Fig. 4). Similar to normal hematopoietic cells, cultured INH CD34$^+$ cells showed a decrease in CD34 expression (Fig. 4a), and INH CD34$^-$ cells did not gain CD34 expression during *ex vivo* culture (Fig. 4b). These data suggest that lines passed in mice were different from cell lines cultured in medium, and that the maintenance of self-renewal activity and the reversibility of CD34 expression need an *in vivo* environment.

Lineage commitment. Southern blot analysis of *IGH* shows rearranged bands (Fig. S2a), which were identical to those of the original samples (data not shown). To analyze the existence of leukemia clones in HSC and progenitors, we determined the CDR-3 sequence and used the leukemia-CDR-3-specific primer to detect leukemia cells in the HSC and progenitor populations (Fig. S2b,c). The expression of MIZ-specific CDR-3 was detected in all fractions (Fig. S2d). Moreover, the expression level was similar in these fractions, indicating the general existence of leukemia cells even in the HSC compartment.

Immunostaining analysis of leukemic mouse BM. To examine where CD34$^+$ leukemia cells localize *in vivo*, sterna of leukemic mice (INH, OMR, MKS, and MIZ) were immunohistochemically examined for human CD34 expression (Fig. 5a). Similar to flow cytometric results, leukemic cells of MKS and MIZ mice were almost positive for CD34. However, INH and OMR BM consisted of both positive and negative cells for CD34 and showed a mosaic-like structure. A sternum of an INH leukemic mouse transplanted with the CD34$^-$ INH cells was stained for human CD45 and CD34 (Fig. 5b). CD34 re-expression from the CD34$^-$ INH cells was also confirmed by immunohistochemical staining. CD34$^+$ cells were scattered and there was no preference of CD34$^+$ cells to the endosteal region.

Discussion

In this study, we transplanted Ph$^+$ leukemia samples into NOG mice, passed leukemia serially, and established six Ph$^+$ leukemia lines *in vivo* in NOG mice. The transplanted and passed leukemia lines reproduced an apparently hierarchical control of CD34/CD38 expression.

Chronic myelogenous leukemia is a myeloproliferative neoplasm that originates from a pluripotent BM HSC with the *BCR-ABL* fusion gene.[20] It is evident that CML originates from an HSC based on the following findings: Ph$^+$ cells are detected in all lineages of peripheral blood; and the *BCR-ABL* fusion gene is detected in the stem cell fraction, even in CML patients in molecular complete remission (CR) due to imatinib treatment.[26,27] However, CML-BC appears to also harbor progenitor cells capable of initiating leukemia.[21,22] The acquisition of additional gene abnormalities is believed to block differentiation and accelerate the self-renewal capacity of these cells.[28,29] Our previous studies and those of others have shown that the GMP-like population is expanded in the CML-BC population,[21,24] and it also expressed CD19/CD10 or CD13. In the current study, we confirmed this finding and showed that CD34$^+$CD38$^-$, CD34$^+$CD34$^+$, or CD34$^-$CD38$^+$ fractions were able to repopulate CML-BC in NOG mice. Transplantation of the CD34$^-$CD38$^+$ fraction resulted in the expansion of a CD34$^-$CD38$^+$ leukemia in the early phase, but later a CD34$^+$CD38$^+$ fraction emerged in the BM and spleen in the INH line. In the OMR line and UPN6 sample, injection of either CD34$^+$ or CD34$^-$ reconstituted the same pattern of CD34/CD38 expression. Similar findings were recently reported, in which the CD34$^-$CD19$^+$ ALL population can self-renew and serially transfer ALL in NOD/SCID mice.[17]

There have been conflicting data published regarding the LSC fraction of ALL. It was reported that the stem cell fraction had either CD34 or CD19 expression. CD133$^+$/CD19$^-$ cells were also shown to have stem cell activity in

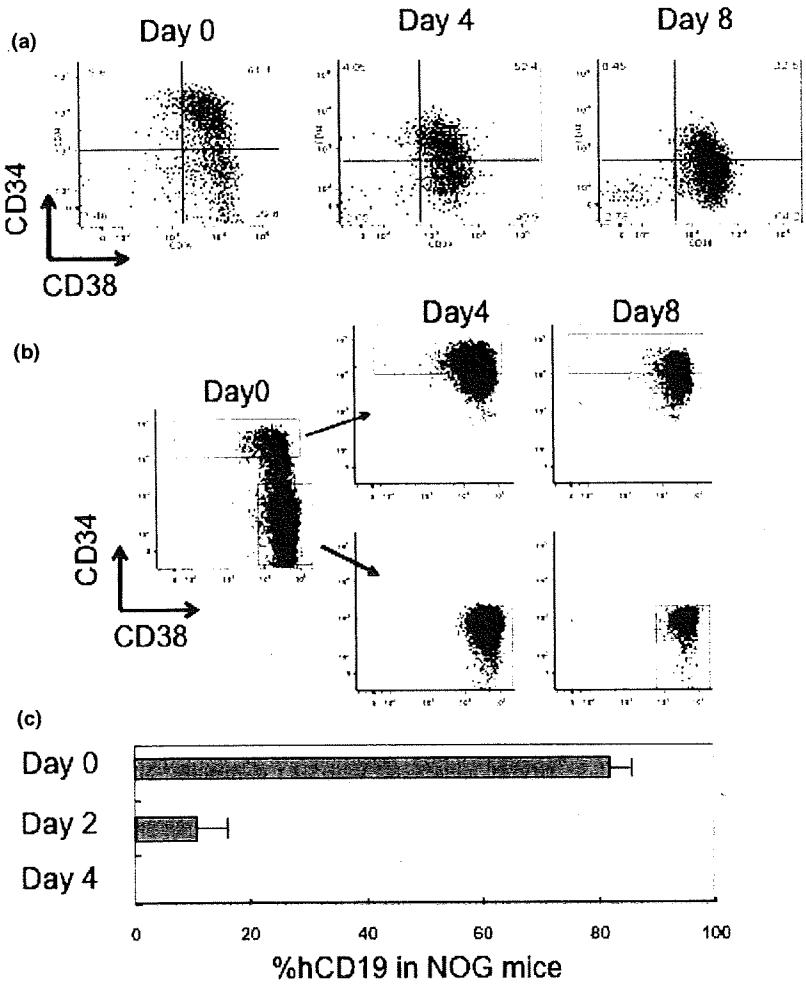

Fig. 4. *In vitro* cultured chronic myelogenous leukemia blast crisis (INH) cells were not transplantable into NOD/SCID mice. Unsorted (a) and sorted (b) INH cells from the bone marrow of primary recipient mice were cultured in serum-free medium containing rhSCF, rhTPO, rhFLT3L, and rhIL-7. Immunophenotypic analysis was carried out at the designated time points. (c) Engrafted INH cells were detected by anti-human CD19 (hCD19) antibody. Cells cultured *in vitro* for more than 2 days were not transplantable into NOD/SCID mice.

precursor-B cell ALL using a NOD/SCID mouse xenotransplantation method.[16] Furthermore, serial transplantation studies indicated that $CD133^+/CD19^-$ ALL cells were capable of self-renewal and expansion of the progenitor cell pool. However, it was also reported that the $CD34^+/CD38^-/CD19^+$ but not the $CD34^+/CD38^+/CD19^+$ fraction repopulated ALL in NOD/SCID mice.[30] Thus, how the expression of CD34, CD38, or CD19 relates to the ALL LSCs remains unclear. It is possible that there is heterogeneity at the stem cell level among ALL cases and that serial transplantation might promote or select for xeno-adaptation. Using the intrafemoral NOD/SCID serial transplantation assay, le Viseur *et al.* described that the leukemia-initiating ability of standard-risk ALL was found in both the $CD34^+CD19^-$ and $CD34^+CD19^+$ populations, and that the $CD34^-CD19^+$ population was able to serially transplant leukemia in high-risk ALL, exclusive of Ph^+ ALL.[17] In Ph^+ ALL, there is a report that only the $CD34^+CD38^-$ fraction can repopulate in NOD/SCID mice and this is in line with the report that a primitive hematopoietic cell is the target for leukemic transformation.[11,1] Our result regarding Ph^+ ALL LSCs is different from the report by Cobaleda *et al.*[11] In our system, not only the $CD34^+CD38^-$ but also $CD34^+CD38^+$ and $CD34^-CD38^+$ fractions can repopulate by transplantation into mice.

This discrepancy is probably due to the mouse strain we used. The more severely immunocompromised NOG mice, which not

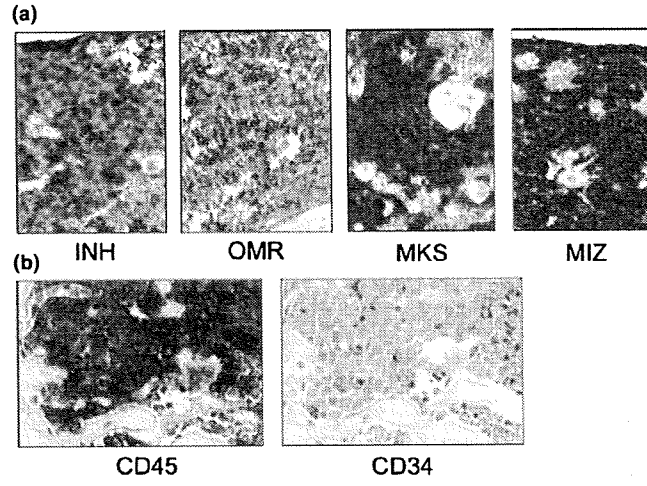

Fig. 5. Immunostaining analysis of leukemic mouse bone marrow. Each leukemic mouse was dissected 8 weeks after transplantation. (a) Sterna of leukemic mice transplanted with unfractionated original leukemia cells (Table 1) were immunohistochemically stained for human CD34. (b) A sternum obtained from a mouse transplanted with $CD34^-$ chronic myelogenous leukemia blast crisis (INH) cells was stained for human CD45 (left panel) and CD34 (right panel).

doi: 10.1111/j.1349-7006.2009.01440.x

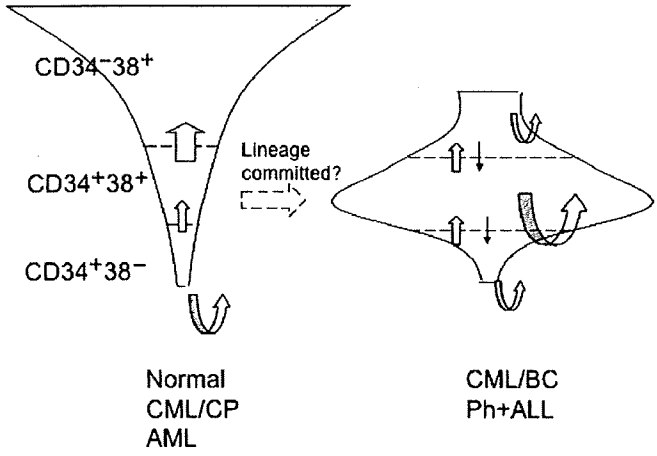

Fig. 6. Summary of Philadelphia chromosome-positive (Ph^+) leukemia stem cells. Differential distribution of the self-renewal populations in normal hematopoiesis (Normal), chronic myelogenous leukemia chronic phase (CML-CP), and acute myeloid leukemia (AML), and CML blast crisis (CML-BC) and Ph^+ acute lymphoblastic leukemia (ALL). In CML-CP and AML, only the $CD34^+CD38^-$ population possesses self-renewal capability but proliferative potential is increased along with shifting from $CD34^+CD38^-$ and $CD34^+CD38^+$ to $CD34^-CD38^+$. In contrast, in CML-BC and Ph^+ ALL, the $CD34^+CD38^-$ population is dominant and has greater self-renewal capability but all compartments can self-renew. Furthermore, leukemia cells of CML-BC and Ph^+ ALL reversibly shift between $CD34^+$ and $CD34^-$. Curved arrow, self-renewal capability; straight arrow, shift between compartments.

only have impaired T cells, B cells and natural killer cells but also impaired complements, macrophages, and dendritic cells, likely permit higher levels of engraftment of human cells than NOD/SCID mice.[25] In our study, the engraftment of the INH $CD34^+$ fraction into NOD/SCID was similar to that seen in NOG mice, whereas the engraftment of $CD34^-$ was unsuccessful. In the OMR line, however, neither $CD34^+$ nor $CD34^-$ fractions were transferred into NOD/SCID mice if 1×10^4 cells were injected. When 1×10^6 OMR cells were transplanted into irradiated NOD/SCID mice, half of the mice received the OMR line (data not shown). These findings suggest that the mouse strain significantly contributes to engraftment of human leukemia cells. Recently, a report by Kong *et al.* has also shown that the $CD34^+/CD38^-/CD19^+$ as well as $CD34^+/CD38^+/CD19^+$ cells are leukemia-initiating cells in human B-precursor ALL using NOG mice.[15] Their results are quite compatible with our data, and to develop and use better humanized mice is preferable, in order to properly evaluate engraftments and reconstitutions.[31]

We then asked whether these Ph^+ leukemia lines were able to be maintained in *ex vivo* culture. Although several culture media were tested with or without murine feeder cells, cell culture was unsuccessful. In general, lymphoid cells are considerably different from myeloid cells whose fate is normally determined only in BM and toward differentiation and death.[32] In contrast, lymphoid cells migrate from BM into lymphoid tissues and mature there. Only a small portion of them can survive from selection and most of them are induced into apoptosis, suggesting the mechanism to control their survival is more complicated.

Although AML LSCs are thought to express CD34 on their surface, it is controversial whether ALL LSCs exist within the $CD34^+$ fraction. In the report by le Viseur *et al.*, both $CD34^+$ and $CD34^-$ fractions of high risk ALL can serially transplant leukemia in immunodeficient mice.[17] Furthermore, both the $CD34^+$ and $CD34^-$ fractions reproduced the original phenotype of CD34 expression in those mice. One explanation for the different CD34 expression in LSCs among leukemias is their lineage. Interestingly, our serial transplantation of $CD34^-$ cells from Ph^+ ALL (OMR) produced both $CD34^+$ and $CD34^-$ cells, and showed a similar CD34 expression pattern to the parental leukemia, which is compatible with le Visueur's result. In contrast, $CD34^-$ cells from CML-BC (INH) produced a limited portion of $CD34^+$ cells and showed a different CD34 expression pattern than the original leukemia. Unlike myeloid cells whose self-renewal is lost during differentiation, mature lymphoid cells survive for a long period and even restart proliferation upon stimulation. This self-renewal capability of lymphoid cells might account for the higher reproducibility of CD34 expression in ALL leukemia cells and, to a lesser extent, in CML-BC, but not in AML. Recent studies suggest that LSCs are responsible for leukemia relapse following conventional or targeted therapies and that eradication of LSCs might be necessary to cure the disease. This Ph^+ leukemia NOG mice model will be useful not only to characterize LSCs but also to develop anti-LSC therapy.

Finally, our study suggested that the leukemia-repopulating capacity of transformed Ph^+ leukemia cells is not restricted by the fractionation of CD34 and CD38, as is the case in AML, but rather that the repopulating ability is associated with the host mouse species, and that CD34 expression is reversible *in vivo* from negative to positive (Fig. 6).

Acknowledgments

This study was supported by Grants-in-Aid from the National Institute of Biomedical Innovation and from the Ministry of Education, Culture, Sports, Science and Technology on Scientific Research, and a Grant-in-Aid for Scientific Research (B) from the Japan Society for the Promotion of Science.

Disclosure Statement

None.

References

1 Bonnet D, Dick JE. Human acute myeloid leukemia is organized as a hierarchy that originates from a primitive hematopoietic cell. *Nat Med* 1997; **3**: 730–737.
2 Pardal R, Clarke MF, Morrison SJ. Applying the principles of stem-cell biology to cancer. *Nat Rev Cancer* 2003; **3**: 895–902.
3 Wang JC, Dick JE. Cancer stem cells: lessons from leukemia. *Trends Cell Biol* 2005; **15**: 494–501.
4 Jordan CT. The leukemic stem cell. *Best Pract Res Clin Haematol* 2007; **20**: 13–18.
5 Krause DS, Van Etten RA. Right on target: eradicating leukemic stem cells. *Trends Mol Med* 2007; **13**: 470–481.
6 Jordan CT, Upchurch D, Szilvassy SJ *et al.* The interleukin-3 receptor alpha chain is a unique marker for human acute myelogenous leukemia stem cells. *Leukemia* 2000; **14**: 1777–1784.
7 Lumkul R, Gorin NC, Malehorn MT *et al.* Human AML cells in NOD/SCID mice: engraftment potential and gene expression. *Leukemia* 2002; **16**: 1818–1826.
8 Hope KJ, Jin L, Dick JE. Acute myeloid leukemia originates from a hierarchy of leukemic stem cell classes that differ in self-renewal capacity. *Nat Immunol* 2004; **5**: 738–743.
9 Ishikawa F, Yoshida S, Saito Y *et al.* Chemotherapy-resistant human AML stem cells home to and engraft within the bone-marrow endosteal region. *Nat Biotechnol* 2007; **25**: 1315–1321.
10 Ninomiya M, Abe A, Katsumi A *et al.* Homing, proliferation and survival sites of human leukemia cells *in vivo* in immunodeficient mice. *Leukemia* 2007; **21**: 136–142.
11 Cobaleda C, Gutierrez-Cianca N, Perez-Losada J *et al.* A primitive hematopoietic cell is the target for the leukemic transformation in human philadelphia-positive acute lymphoblastic leukemia. *Blood* 2000; **95**: 1007–1013.

12 George AA, Franklin J, Kerkof K *et al.* Detection of leukemic cells in the CD34(+)CD38(−) bone marrow progenitor population in children with acute lymphoblastic leukemia. *Blood* 2001; **97**: 3925–3930.
13 Cox CV, Evely RS, Oakhill A, Pamphilon DH, Goulden NJ, Blair A. Characterization of acute lymphoblastic leukemia progenitor cells. *Blood* 2004; **104**: 2919–2925.
14 Castor A, Nilsson L, Astrand-Grundstrom I *et al.* Distinct patterns of hematopoietic stem cell involvement in acute lymphoblastic leukemia. *Nat Med* 2005; **11**: 630–637.
15 Kong Y, Yoshida S, Saito Y *et al.* $CD34^+$ $CD38^+$ $CD19^+$ as well as $CD34^+$ CD38− $CD19^+$ cells are leukemia-initiating cells with self-renewal capacity in human B-precursor ALL. *Leukemia* 2008; **22**: 1207–1213.
16 Cox CV, Diamanti P, Evely RS, Kearns PR, Blair A. Expression of CD133 on leukemia-initiating cells in childhood ALL. *Blood* 2009; **113**: 3287–3296.
17 le Viseur C, Hotfilder M, Bomken S *et al.* In childhood acute lymphoblastic leukemia, blasts at different stages of immunophenotypic maturation have stem cell properties. *Cancer Cell* 2008; **14**: 47–58.
18 Bernt KM, Armstrong SA. Leukemia stem cells and human acute lymphoblastic leukemia. *Semin Hematol* 2009; **46**: 33–38.
19 Heidenreich O, Vormoor J. Malignant stem cells in childhood ALL: the debate continues! *Blood* 2009; **113**: 4476–4477; author reply 4477.
20 Ren R. Mechanisms of BCR-ABL in the pathogenesis of chronic myelogenous leukemia. *Nat Rev Cancer* 2005; **5**: 172–183.
21 Jamieson CH, Ailles LE, Dylla SJ *et al.* Granulocyte-macrophage progenitors as candidate leukemic stem cells in blast-crisis CML. *N Engl J Med* 2004; **351**: 657–667.
22 Abrahamsson AE, Geron I, Gotlib J *et al.* Glycogen synthase kinase 3beta missplicing contributes to leukemia stem cell generation. *Proc Natl Acad Sci U S A* 2009; **106**: 3925–3929.
23 Ito M, Hiramatsu H, Kobayashi K *et al.* NOD/SCID/gamma(c)(null) mouse: an excellent recipient mouse model for engraftment of human cells. *Blood* 2002; **100**: 3175–3182.
24 Abe A, Minami Y, Hayakawa F *et al.* Retention but significant reduction of BCR-ABL transcript in hematopoietic stem cells in chronic myelogenous leukemia after imatinib therapy. *Int J Hematol* 2008; **88**: 471–475.
25 Kiyoi H, Naoe T, Horibe K, Ohno R. Characterization of the immunoglobulin heavy chain complementarity determining region (CDR)-III sequences from human B cell precursor acute lymphoblastic leukemia cells. *J Clin Invest* 1992; **89**: 739–746.
26 Elrick LJ, Jorgensen HG, Mountford JC, Holyoake TL. Punish the parent not the progeny. *Blood* 2005; **105**: 1862–1866.
27 O'Hare T, Corbin AS, Druker BJ. Targeted CML therapy: controlling drug resistance, seeking cure. *Curr Opin Genet Dev* 2006; **16**: 92–99.
28 Mullighan CG, Miller CB, Radtke I *et al.* BCR-ABL1 lymphoblastic leukaemia is characterized by the deletion of Ikaros. *Nature* 2008; **453**: 110–114.
29 Calabretta B, Perrotti D. The biology of CML blast crisis. *Blood* 2004; **103**: 4010–4022.
30 Hong D, Gupta R, Ancliff P *et al.* Initiating and cancer-propagating cells in TEL-AML1-associated childhood leukemia. *Science* 2008; **319**: 336–339.
31 Shultz LD, Ishikawa F, Greiner DL. Humanized mice in translational biomedical research. *Nat Rev Immunol* 2007; **7**: 118–130.
32 Metcalf D. Hematopoietic cytokines. *Blood* 2008; **111**: 485–491.

Supporting Information

Additional Supporting Information may be found in the online version of this article:

Fig. S1. Purity analyses of sorted cells. Chronic myelogenous leukemia blast crisis (INH) cells were sorted by FACSAria according to CD34/CD38 expression. The purities of sorted cells were more than 98%.

Fig. S2. Analysis of *IGH* rearrangements in leukemia lines and detection of (complementarity-determining region-3) CDR-3 sequence in hematopoietic stem cells (HSCs)/progenitors from MIZ (Table 1). (a) Southern blot analysis of genomic DNA from INH, MKS, and MIZ. Red arrows indicate rearranged bands. (b) Nucleotide sequence of *IGH* CDR-3 of MIZ. Location of the oligonucleotide primers is shown. (c) HSC/progenitor profiles of MIZ. Granulocyte/monocyte progenitor (GMP)-like population was prominent. CMP, common myeloid progenitor; IL, interleukin; MEP, megakaryocyte/erythroid progenitor; Thy1, CD90. (d) Detection of CDR-3 in HSC/progenitors from MIZ. Expression of leukemia-specific CDR-3 was detected in all fractions at a similar level. The amounts of cDNA for PCR amplification were standardized by the value of real-time quantitative PCR data of *GAPDH*.

doi: 10.1111/j.1349-7006.2009.01440.x

Biochemical and Biophysical Research Communications 390 (2009) 48–53

Contents lists available at ScienceDirect

Biochemical and Biophysical Research Communications

journal homepage: www.elsevier.com/locate/ybbrc

Escape mechanisms from antibody therapy to lymphoma cells: Downregulation of *CD20* mRNA by recruitment of the HDAC complex and not by DNA methylation

Takumi Sugimoto [a], Akihiro Tomita [a,*], Junji Hiraga [a,b], Kazuyuki Shimada [a], Hitoshi Kiyoi [c], Tomohiro Kinoshita [a], Tomoki Naoe [a]

[a] *Department of Hematology and Oncology, Nagoya University Graduate School of Medicine, Nagoya, Japan*
[b] *Department of Hematology, Toyota Memorial Hospital, Toyota, Japan*
[c] *Department of Infectious Diseases, Nagoya University School of Medicine, Nagoya, Japan*

ARTICLE INFO

Article history:
Received 15 September 2009
Available online 19 September 2009

Keywords:
CD20
Rituximab
Epigenetics
Histone deacetylases
DNA methytransferases

ABSTRACT

Although rituximab is a critical monoclonal antibody therapy for CD20-positive B-cell lymphomas, rituximab resistance showing a CD20-negative phenotypic change has been a considerable clinical problem. Here we demonstrate that *CD20* mRNA and protein expression is repressed by recruitment of a histone deacetylase protein complex to the *MS4A1* (*CD20*) gene promoter in CD20-negative transformed cells after treatment with rituximab. *CD20* mRNA and protein expression were stimulated by decitabine (5-Aza-dC) in CD20-negative transformed cells, and was enhanced by trichostatin A (TSA). Immunoblotting indicated that DNMT1 expression was first downregulated 1 day after treatment with 5-Aza-dC, but IRF4 and Pu.1, the transcriptional regulators of *MS4A1*, were still expressed with or without 5-Aza-dC. Interestingly, CpG methylation of the *MS4A1* promoter was not observed in CD20-negative transformed cells without 5-Aza-dC. A chromatin immunoprecipitation (ChIP) assay indicated that the Sin3A–HDAC1 co-repressor complex was recruited to the promoter and dissociated from the promoter with 5-Aza-dC and TSA, resulting in histone acetylation. Under these conditions, IRF4 and Pu.1 were continually recruited to the promoter with or without 5-Aza-dC and TSA. These results suggest that recruitment of the Sin3A–HDAC1 complex is related to downregulation of CD20 expression in CD20-negative B-cells after treatment with rituximab.

Introduction

Rituximab is the first therapeutic monoclonal antibody targeting human malignant tumors, and is now an indispensable molecular-targeting drug for CD20-positive B-cell lymphomas [1–3]. Although the effectiveness is significant, resistance to rituximab has also become a considerable problem [4].

Several mechanisms of the resistance have been suggested, including loss of CD20 protein expression after rituximab use [5–12] and CD20 gene mutations [13]. Furthermore, other mechanisms have also been suggested [4] such as internalization of CD20 protein [14], interference with accessibility of rituximab to CD20 protein by inhibitory factors, rapid metabolism of the antibody, abnormalities in B-cell signaling in tumor cells [15], abnormalities of apoptosis [16], antibody-dependent cell-mediated cytotoxicity (ADCC), and complement-dependent cytotoxicity (CDC) [17].

Very recently, we reported observation of downregulation of CD20 protein expression in CD20-positive B-cell lymphoma patients after treatment with rituximab-containing combination chemotherapies [6,7]. In those cases, it was strongly suggested that aberrant downregulation of *MS4A1* expression was closely related to the loss of CD20 protein expression, and that expression of CD20 and rituximab sensitivity were partially restored by some molecular-targeting drugs [6,7]. Although these findings suggest that epigenetic mechanisms, in part, contribute to the downregulation of CD20 expression, the molecular mechanisms are still not clear. Furthermore, a recent report indicated that reduced CD20 protein expression in *de novo* diffuse large B-cell lymphoma is associated with a poor survival rate [18]. Thus, understanding the mechanisms of downmodulation of CD20 protein expression is likely to be very important from both basic research and clinical viewpoints.

In this report, we show that the recruitment of a histone deacetylase (HDAC) co-repressor complex to the *MS4A1* promoter

* Corresponding author. Address: Department of Hematology and Oncology, Nagoya University Graduate School of Medicine, Tsurumai-Cho 65, Showa-ku, Nagoya 466-8560, Japan. Fax: +81 52 744 2161.
E-mail address: atomita@med.nagoya-u.ac.jp (A. Tomita).

0006-291X/$ - see front matter © 2009 Elsevier Inc. All rights reserved.
doi:10.1016/j.bbrc.2009.09.059

region, but not DNA methylation [19], is involved in CD20-negative phenotypic changes in B-cell lymphoma cells after treatment with rituximab. We show that the complex dissociated from the promoter in the presence of a DNA methyltransferase (DNMT) inhibitor and a HDAC inhibitor [20], resulting in partial restoration of CD20 expression.

Materials and methods

Cell culture conditions and treatment with epigenetic drugs. RRBL1 [6], Raji, and NALM6 cells were cultured in RPMI 1640 medium (Sigma–Aldrich, St. Louis, MO, USA) with 10% fetal calf serum. Five-Aza-dC (5-aza-2′-deoxycytidine; Sigma, St. Louis, MO) and TSA (Sigma) at final concentrations of 100 μM and 100 nM, respectively, were added directly to the culture medium.

Immunoblotting. Cells (~5 × 10^5) were lysed in 100 μl of lysis buffer (50 mM Tris–HCl, pH 8.0, 1.5 mM $MgCl_2$, 1 mM EGTA, 5 mM KCl, 10% glycerol, 0.5% NP-40, 300 mM NaCl, 0.2 mM PMSF, 1 mM DTT, and a complete mini protease inhibitor tablet (Roche)). After centrifugation at 10,000 *g* for 10 min, the supernatants were placed in new tubes, and 100 μl of 2× SDS sample buffer was added. After boiling for 5 min, samples were separated with SDS–polyacrylamide gel electrophoresis (SDS–PAGE). Immunoblotting was carried out as described previously [21,22] using anti-CD20, -IRF4, -Pu.1, -GAPDH antibodies (Santa Cruz Biotechnology, Santa Cruz, CA, USA), and anti-DNMT1 antibody (Abcam, Cambridge, MA, USA).

RNA preparation and reverse transcriptase-polymerase chain reaction (RT-PCR). RNA from cell lines (1 × 10^5 cells) was obtained using Trizol (Invitrogen, Carlsbad, CA, USA). Complementary DNA (cDNA) was prepared as reported previously [7,22].

For RT-PCR, the following primers were designed: CD20-U; 5′-ATGAAAGGCCCTATTGCTATG-3′, CD20-L; 5′-GCTGGTTCACAGTTGTATATG-3′, β-actin-U; 5′-TCACTCATGAAGATCCTCA-3′, and β-actin-L; 5′-TTCGTGGATGCCACAGGAC-3′. Semi-quantitative RT-PCR with AmpliTaq Gold was performed as described previously [6].

Methylation status of the MS4A1 promoter. To examine the methylation status, bisulfite sequencing was performed. Genomic DNA was prepared with a QIAamp DNA Blood Mini kit (Qiagen, Valencia, CA, USA). Bisulfite treatment was performed using EpiTect Bisulfite kits (Qiagen). After bisulfite treatment, PCR of the *MS4A1* promoter was performed using the specific primers as follows, MS4A1-pro-MSPU; 5′-GGTAGTATGAGTATGTTAGGTAGTT-3′, MS4A1-pro-MSPL; 5′-TTTTCCTTACCTAAATCTCCAAAA-3′. PCR fragments were cloned into a pGEM-T easy vector (Promega, Madison, WI, USA) and sequenced.

Flow cytometry (FCM) analysis. Cell surface antigens of RRBL1 with or without 5-Aza-dC and TSA treatment were analyzed using a BD FACSCalibur Flow Cytometer (BD Bioscience, Franklin Lakes, NJ, USA) with anti-CD20 antibody (Leu-16 PE, BD) and mouse IgG1 κ isotype control (PE-Cy7, BD).

Chromatin immunoprecipitation (ChIP) assay. The ChIP assay was performed as described previously [22,23]. For immunoprecipitation (IP), the following antibodies were used; anti-Pu.1, -IRF4 (Santa Cruz Biotechnology), -acetylated H4 (Millipore, Billerica, MA, USA), -Sin3A, and anti-HDAC1 (Abcam) antibodies. Immunoprecipitated DNA was used for semi-quantitative PCR using LA-Taq polymerase (TAKARA, Ohtsu, Japan). The following primers for the *MS4A1* promoter and 3′-intron sequence (negative control) were used; CD20pro-U; 5′-CTAAAAGTGAAGCCAGAAGG-3′, CD20pro-L; 5′-GGAGGGTGAGTGGTGTAGT-3′, CD20-3′U; 5′-GCTGACCTCACATAACTCCT-3′, CD20-3′L; 5′-GAAATCCCTCAGACTCAGAC-3′.

Immunoprecipitation (IP) assay. The IP assay was carried out as described previously [22]. Whole cell lysate was obtained from RRBL1 cells (1 × 10^7) using 800 μl of lysis buffer. After adding 800 μl of lysis buffer without NP-40 and NaCl, the lysate was divided into four tubes (400 μl each) and IP using anti-IRF4, -Sin3A, and -HDAC1 antibodies was performed. The precipitated samples were applied to SDS–PAGE followed by immunoblotting. For the pre-IP samples, 5% of the whole cell lysate was used.

Results

CD20 protein and mRNA expression were stimulated by treatment with 5-Aza-dC in CD20-negative transformed cells

As we reported previously [6,7], the downregulation of CD20 protein and mRNA expression has been observed in some CD20-positive B-cell lymphoma patients after treatment with rituximab-containing chemotherapies. We also reported that the downregulation of CD20 expression was partially stimulated by treatment with the epigenetic drugs 5-Aza-dC and TSA. RRBL1 cells were established from a patient with B-cell lymphoma who showed a CD20-negative phenotypic change after treatment with rituximab [6]. To examine the mechanisms of stimulation of CD20 expression by 5-Aza-dC, we examined the protein expression pattern that may affect CD20 gene transcription in RRBL1 cells. RRBL1 cells were treated with 5-Aza-dC for 24 h, and were then washed and incubated for up to 7 days (Fig. 1A). During this procedure, the cells were harvested several times as indicated and analyzed using semi-quantitative RT-PCR and immunoblotting (IB) (Fig. 1B). *CD20* mRNA and protein expression were stimulated by 5-Aza-dC, and the peak of expression was observed around day 3 after treatment with 5-Aza-dC (lane 6). After day 5, CD20 protein expression had gradually decreased. DNMT1 depletion was confirmed at 24 h after treatment with 5-Aza-dC (lane 4) as reported previously [24]. IRF4 and Pu.1 are transcription factors that interact with the *MS4A1* promoter and regulate CD20 expression [25]. IRF4/Pu.1 was almost constantly expressed throughout the 5-Aza-dC treatment duration (lanes 3–8), but only a modest upregulation was observed after treatment with 5-Aza-dC around day 2 (lane 5). These results suggested that DNMT1 depletion by 5-Aza-dC may be related to stimulation of *MS4A1* expression.

DNA methylation status of the MS4A1 promoter

To explain the activation of *CD20* mRNA and protein expression after treatment with 5-Aza-dC in RRBL1 cells, we next examined the CpG methylation status of the *MS4A1* promoter (Fig. 1C). Interestingly, CpG islands were not observed on the promoter region located ~5 kb upstream from the transcription start site, and only four CG sites were found on the promoter from the −1000 to +100 region. Bisulfite sequencing was carried out to confirm methylated CpG. As shown in Fig. 1C, no CpG methylation was observed on the three CpG sites around the transcription start site in RRBL1 cells. In NALM6 cells, a CD20-negative lymphoblastic leukemia cell line, several methylated CpGs were observed. Furthermore, the same analysis was performed using primary tumor cells from a patient suffering from CD20-negative transformed B-cell lymphoma after treatment with rituximab-containing combination chemotherapies. (Detailed information about this patient is described in our previous paper as UPN3 [7]). The three CpG sites were not methylated, as observed in RRBL1 cells (Fig. 1C, UPN3). These results suggest that transcriptional activation of *MS4A1* by 5-Aza-dC may not be regulated by its promoter CpG demethylation in RRBL1 cells.

Histone deacetylase inhibitor TSA enhances CD20 expression by 5-Aza-dC in CD20-negative transformed cells

Next, we analyzed the effect of a HDAC inhibitor in addition to 5-Aza-dC on *MS4A1* expression in RRBL1 cells. CD20 protein expression in RRBL1 cells was confirmed using immunoblotting

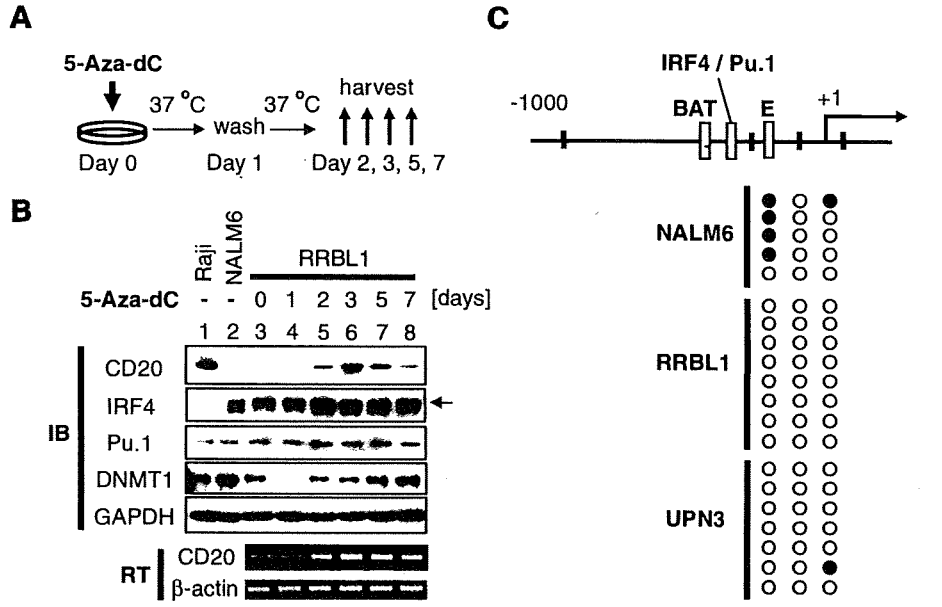

Fig. 1. CD20 protein and mRNA expression were transiently stimulated by treatment with a DNMT inhibitor. (A) Schematic representation of 5-Aza-dC treatment of the CD20-negative transformed B-lymphoma cells. RRBL1 cells were incubated at 37 °C for 24 h, and then washed twice with RPMI medium with 10% FCS without 5-Aza-dC. Cells were further incubated for up to 7 days, and were harvested at days 1, 2, 3, 5, and 7. (B) Protein expression was examined using immunoblotting (IB) with the indicated antibodies. The mRNA expression level was determined using semi-quantitative RT-PCR (RT). The black arrow indicates the band for IRF4. Raji and NALM6 cells were used as positive and negative controls, respectively. GAPDH and β-actin were measured as internal controls. (C) The structure of the *MS4A1* promoter near the transcription start site (from −1000 to +100) is depicted. The BAT-box, IRF4/Pu.1 binding sites, and E-box are shown as shaded boxes. Only four CpG sites, which are putative methylation sites, were found and are shown as black vertical bars. The methylation status of the three CpG sites around the transcription start site in NALM6, RRBL1, and primary B-lymphoma cells that show CD20-negative transformation was analyzed with bisulfite sequencing. Five to eight clones were analyzed from each sample. Black and open circles indicate methylated and non-methylated CpGs, respectively.

and flow cytometry (FCM) (Fig. 2A and B) following treatment with 5-Aza-dC and/or TSA. When RRBL1 cells were treated with 5-Aza-dC or TSA alone, minimal activation of CD20 protein expression was observed using immunoblotting (Fig. 2A, lanes 4 and 5) and FCM (Fig. 2B, 5-Aza-dC). In the presence of 5-Aza-dC and TSA, CD20 protein expression was significantly increased (Fig. 2A, lane 6, and B, 5-Aza-dC + TSA). These results suggested that *MS4A1* expression is, in part, regulated by epigenetic mechanisms such as histone modification including lysine acetylation, rather than DNA CpG methylation of the *MS4A1* promoter.

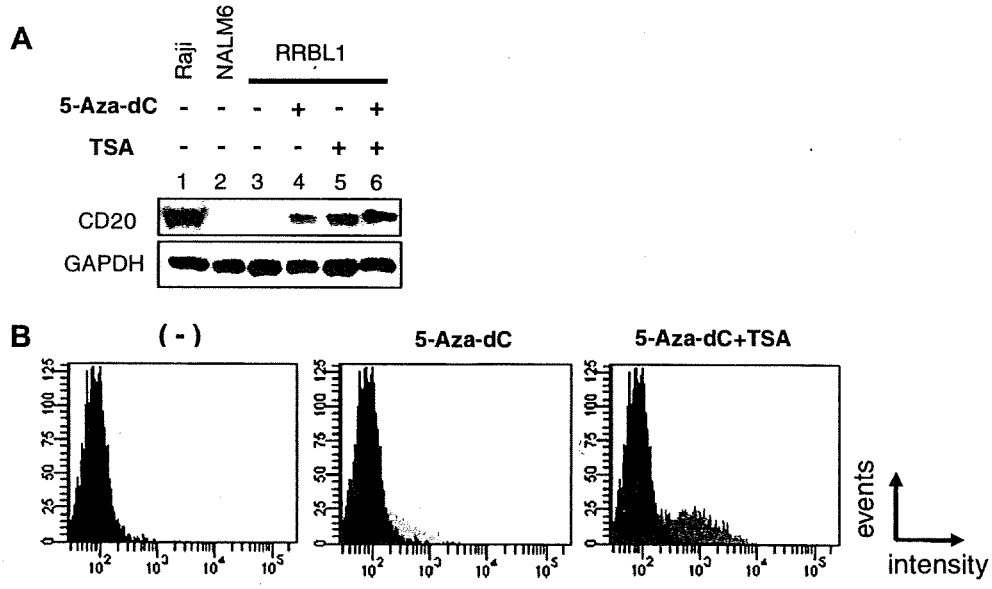

Fig. 2. CD20 protein expression by 5-Aza-dC was enhanced by TSA. CD20 protein expression was shown with IB (A) and FCM (B) with or without epigenetic drugs. For 5-Aza-dC treatment, RRBL1 cells were incubated with 5-Aza-dC for 24 h followed by washing and two additional days of incubation. TSA was added at the start of day 3, and cells were incubated for 24 h. If cells were not treated with 5-Aza-dC, washing was also carried out at day 1 to adjust the incubation conditions. All the cells were harvested at day 4 and utilized for IB and FCM analyses. The untreated and treated cells with the epigenetic drugs were depicted as black and gray areas, respectively (B).

Recruitment of co-repressor proteins and histone deacetylation on the MS4A1 promoter in the absence of epigenetic drugs

To study the molecular mechanisms of transcriptional repression of *MS4A1*, a ChIP assay was performed. RRBL1 cells were incubated with or without 5-Aza-dC and TSA, and a ChIP assay was carried out using anti-Pu.1, -IRF4, -Sin3A, -HDAC1, and -acetylated-histone H4 antibodies. After IP, precipitated genomic DNA was utilized in semi-quantitative PCR using primers for the *MS4A1* promoter (Fig. 3A) and the 3′-intron sequences as a negative control. IRF4 and Pu.1 interactions were consistently observed on the promoter region, but not on the 3′-intron region (Fig. 3B, lanes 5–8). Sin3A and HDAC1, which form a transcription repressor protein complex [26], interacted with the promoter region only in the absence of 5-Aza-dC and TSA (Fig. 3B, lanes 11 and 13). Acetylated-histone H4 was observed at the promoter region with 5-Aza-dC and TSA, but the acetylation was decreased in the absence of the two drugs (lane 9). In the 3′-intron region, histone acetylation was consistently observed with or without 5-Aza-dC and TSA. These results strongly suggest that the Sin3A–HDAC1 co-repressor complex may be recruited to the *MS4A1* promoter through some transcription factors in the absence of epigenetic drugs, resulting in histone deacetylation and transcriptional repression. In addition, the recruitment may be dissociated from the promoter by adding 5-Aza-dC and TSA, resulting in histone acetylation and transcription activation.

The Sin3A–HDAC1 co-repressor complex is found in RRBL1 cells with or without epigenetic drugs

To show that loss of Sin3A–HDAC1 interaction with the *MS4A1* promoter was due to protein complex dissociation and not degradation, we confirmed the protein expression in RRBL1 cells with and without epigenetic drugs using IB. As shown in Fig. 4A, HDAC1 and Sin3A protein expression levels did not change in the presence of epigenetic drugs. Next, we performed an IP assay using anti-IRF4, -Sin3A, and -HDAC1 antibody to confirm that Sin3A and HDAC1 exist as a protein complex, and to examine whether the Sin3A–HDAC1 co-repressor complex was recruited by IRF4 in the absence of epigenetic drugs. The Sin3A–HDAC1 interaction was confirmed with an IP assay using anti-Sin3A and -HDAC1 antibodies (Fig. 4B, lanes 4 and 5), but interaction of IRF4 with this complex was not observed (lane 3). These results indicate that the Sin3A–HDAC1 complex exists in RRBL1 cells with or without 5-Aza-dC and TSA, and that the recruitment of the complex to the *MS4A1* promoter may not involve a direct interaction with IRF4.

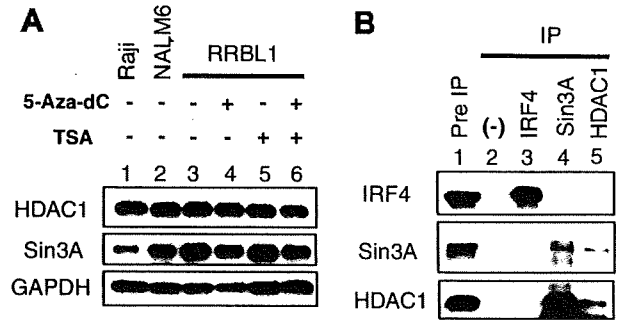

Fig. 4. The Sin3A–HDAC1 co-repressor complex is stably expressed in RRBL1 cells with or without 5-Aza-dC and/or TSA. (A) IB was performed using the RRBL1 lysate after treatment with 5-Aza-dC and/or TSA. Raji and NALM6 cells were used as expression controls. Similar levels of expression of HDAC1 and Sin3A were observed in each sample. (B) Whole cell lysate of RRBL1 cells was obtained using lysis buffer. Lysates were divided into four samples and used for IP using anti-IRF4, -Sin3A, and -HDAC1 antibodies. Five percent of the whole cell lysate was used for the pre-IP samples (lane 1). As a negative control, antibodies for IP were omitted (lane 2). IB indicated that endogenous Sin3A–HDAC1 interacted in RRBL1 cells without epigenetic drugs, but significant interaction with IRF4 was not observed in this assay system.

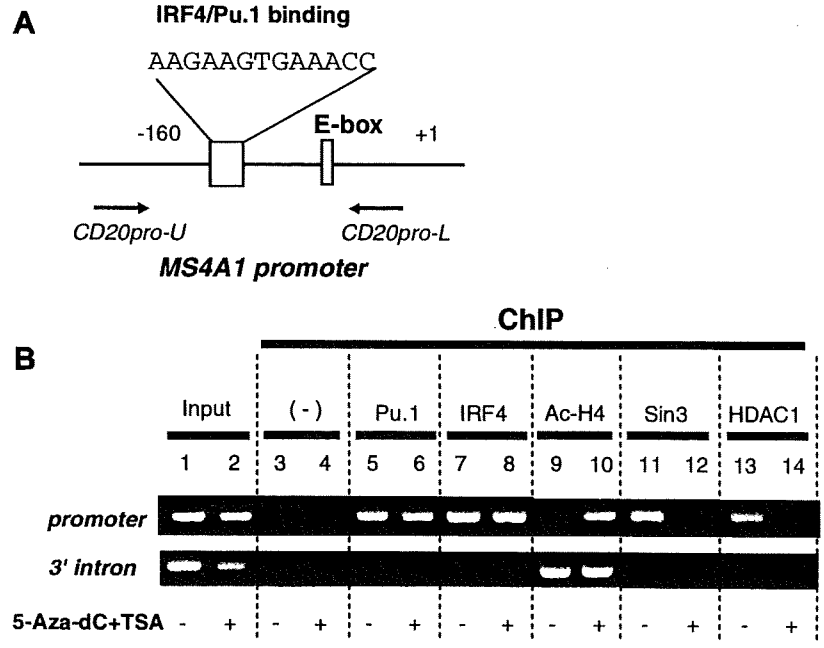

Fig. 3. ChIP assay of the *MS4A1* promoter. The primer set used for amplification of the *MS4A1* promoter (−160 to +1) is shown in (A). The positions of the upper and lower primers are indicated as black arrows. (B) A ChIP assay using anti-Pu.1, -IRF4, -Sin3A, -HDAC1, and -acetylated-histone H4 was performed using the cell lysate from cells treated with or without 5-Aza-dC and TSA. Semi-quantitative PCR was performed, and the amplified DNA fragments were visualized by 1.5% agarose gel electrophoresis. As a positive control, lysate without the IP step was used (input). A ChIP sample without antibodies was used as a negative control (−). PCR using the primers for the 3′-intron region of *MS4A1* was also used as a control. Sin3A and HDAC1 recruitment to the promoter was observed in lanes 11 and 13, and accumulation of histone deacetylation was seen in lane 9.

Discussion

In clinical practice, CD20 expression abnormalities have been reported. Johnson et al. [18] reported that 43 out of 272 (16%) patients with diffuse large B-cell lymphoma (DLBCL) showed reduced CD20 expression using FCM analysis at the time of initial diagnosis, and that the survival rate of this phenotype was significantly lower than that of patients with CD20-positive phenotype. Furthermore, we previously reported that a CD20-negative phenotypic change after using rituximab resulted in resistance to salvage chemotherapies with or without rituximab [6,7]. We observed that all of these patients died of disease progression within 1 year after the diagnosis of CD20-negative transformation, suggesting that the CD20-negative phenotype may be related to the poor prognosis. From these findings, we realized the importance of investigating the mechanisms of downmodulation of CD20 expression to explore overcoming strategies including salvage combination chemotherapies with anti-CD20 antibodies.

In this study, we firstly investigated the effect of 5-Aza-dC on RRBL1 cells. DNMT1 protein reduction was observed 1 day after adding 5-Aza-dC, followed by temporal upregulation of CD20 protein expression (Fig. 1B). This phenomenon suggested that CpG demethylation of the *MS4A1* promoter region was a result of DNMT1 depletion. But interestingly, significant CpG islands were not located at the promoter, suggesting that *MS4A1* activation by 5-Aza-dC was not regulated directly by *MS4A1* promoter methylation.

The next hypothesis we investigated was that expression of transcription factors, which is critical for *MS4A1* expression, was regulated by the methylation status of the promoter DNA. We analyzed the protein expression level of IRF4/Pu.1, and only a modest upregulation was observed. Furthermore, the ChIP assay showed that IRF4/Pu.1 recruitment to the *MS4A1* promoter was fairly stable in the presence or absence of 5-Aza-dC and TSA (Fig. 3B). On the other hand, Sin3A–HDAC1 recruitment and histone deacetylation was observed in the absence of epigenetic drugs. Because previous reports have indicated that HDACs form large protein complexes, such as Sin3 [26], NuRD/Mi-2 [27], and N-CoR/SMRT co-repressor complexes [26,28], and are recruited to the specific promoter by transcription factors, we analyzed whether the Sin3A–HDAC1 complex interacts with IRF4 in RRBL1 cells. Using an IP assay, we observed that HDAC1 interacts with Sin3A but not with IRF4 (Fig. 4B). We also analyzed the recruitment of the proteins N-CoR, HDAC3, and TBLR1 (transducin β-like protein 1 relating protein), which are all expressed in the same co-repressor complex *in vivo* [21–23,26,28], to the promoter region using the ChIP assay. Significant recruitment of these proteins was not seen in this assay (data not shown).

Thus, these findings suggest that, (1) *MS4A1* repression is not directly regulated by methylation of its promoter and (2) transcription factors other than IRF4 recruit the Sin3A–HDAC1 co-repressor complex to the *MS4A1* promoter to repress transcription through histone deacetylation. Our previous report [6] showed that treatment with TSA without 5-Aza-dC upregulates CD20 expression in RRBL1 cells within 1 day, suggesting that the activity of HDAC may be more critical for *MS4A1* expression than the activity of DNMTs. One explanation for why 5-Aza-dC can stimulate *MS4A1* expression is that the expression of some transcription factors, whose expression is critical for CD20 expression, may be regulated by CpG methylation of the gene promoters. The maximal effect of 5-Aza-dC on CD20 protein expression was seen at 3 days after treatment with 5-Aza-dC, which is consistent with this hypothesis. The knockdown of endogenous DNMT1 using the siRNA technique may help explain the importance of DNMT1 for *MS4A1* repression. On the other hand, the possibility that CpG islands in *MS4A1* that affect its expression are in a location that is relatively remote (~5 kb) from the transcription start site cannot be excluded. Further investigation is needed.

In our study, the efficiency of stimulating CD20 protein expression in CD20-negative transformed cells using epigenetic drugs is not complete (Fig. 2B). As we showed previously [7], this efficiency may not be sufficient to overcome resistance to rituximab. Using the newer generation humanized-anti-CD20 monoclonal antibodies, such as ofatumumab [29], GA-101 [30], and others, which have higher antibody binding capacity with CD20 and/or a higher CDC/ADCC activity, may help overcome the resistance. We also anticipate the use of those therapies in combination with epigenetic drugs such as HDAC and/or DNMT inhibitors. Further investigation is still needed.

Acknowledgments

This work is supported in part by a Grant-in-Aid for Cancer Research (21-6-3) from the Ministry of Health, Labor and Welfare, a Grant-in-Aid from the National Institute of Biomedical Innovation, and a Grant-in-Aid in Scientific Research (20591116) from the Ministry of Education, Culture, Sports, Science and Technology, Japan. We thank Dr. Shinsuke Iida for providing critical information about IRF4. We also thank Akihide Atsumi, Tomoka Wakamatsu, Yukie Konishi, Mari Otsuka, Eriko Ushida, and Chieko Kataoka for valuable laboratory assistance.

References

[1] B.D. Cheson, Monoclonal antibody therapy for B-cell malignancies, Semin. Oncol. 33 (2006) S2–S14.
[2] B. Coiffier, E. Lepage, J. Briere, R. Herbrecht, H. Tilly, R. Bouabdallah, P. Morel, E. Van Den Neste, G. Salles, P. Gaulard, F. Reyes, P. Lederlin, C. Gisselbrecht, CHOP chemotherapy plus rituximab compared with CHOP alone in elderly patients with diffuse large-B-cell lymphoma, N. Engl. J. Med. 346 (2002) 235–242.
[3] B.D. Cheson, J.P. Leonard, Monoclonal antibody therapy for B-cell non-Hodgkin's lymphoma, N. Engl. J. Med. 359 (2008) 613–626.
[4] M.R. Smith, Rituximab (monoclonal anti-CD20 antibody): mechanisms of action and resistance, Oncogene 22 (2003) 7359–7368.
[5] M.S. Czuczman, S. Olejniczak, A. Gowda, A. Kotowski, A. Binder, H. Kaur, J. Knight, P. Starostik, J. Deans, F.J. Hernandez-Ilizaliturri, Acquirement of rituximab resistance in lymphoma cell lines is associated with both global CD20 gene and protein down-regulation regulated at the pretranscriptional and posttranscriptional levels, Clin. Cancer Res. 14 (2008) 1561–1570.
[6] A. Tomita, J. Hiraga, H. Kiyoi, M. Ninomiya, T. Sugimoto, M. Ito, T. Kinoshita, T. Naoe, Epigenetic regulation of CD20 protein expression in a novel B-cell lymphoma cell line, RRBL1, established from a patient treated repeatedly with rituximab-containing chemotherapy, Int. J. Hematol. 86 (2007) 49–57.
[7] J. Hiraga, A. Tomita, T. Sugimoto, K. Shimada, M. Ito, S. Nakamura, H. Kiyoi, T. Kinoshita, T. Naoe, Down-regulation of CD20 expression in B-cell lymphoma cells after treatment with rituximab-containing combination chemotherapies: its prevalence and clinical significance, Blood 113 (2009) 4885–4893.
[8] T. Sonoki, Y. Li, S. Miyanishi, H. Nakamine, N. Hanaoka, H. Matsuoka, I. Mori, H. Nakakuma, Establishment of a novel CD20 negative mature B-cell line, WILL2, from a CD20 positive diffuse large B-cell lymphoma patient treated with rituximab, Int. J. Hematol. 89 (2009) 400–402.
[9] I. Jilani, S. O'Brien, T. Manshuri, D.A. Thomas, V.A. Thomazy, M. Imam, S. Naeem, S. Verstovsek, H. Kantarjian, F. Giles, M. Keating, M. Albitar, Transient down-modulation of CD20 by rituximab in patients with chronic lymphocytic leukemia, Blood 102 (2003) 3514–3520.
[10] T. Kinoshita, H. Nagai, T. Murate, H. Saito, CD20-negative relapse in B-cell lymphoma after treatment with rituximab, J. Clin. Oncol. 16 (1998) 3916.
[11] T.A. Davis, D.K. Czerwinski, R. Levy, Therapy of B-cell lymphoma with anti-CD20 antibodies can result in the loss of CD20 antigen expression, Clin. Cancer Res. 5 (1999) 611–615.
[12] A.J. Ferreri, G.P. Dognini, C. Verona, C. Patriarca, C. Doglioni, M. Ponzoni, Reoccurrence of the CD20 molecule expression subsequent to CD20-negative relapse in diffuse large B-cell lymphoma, Haematologica 92 (2007) e1–e2.
[13] Y. Terui, Y. Mishima, N. Sugimura, K. Kojima, T. Sakurai, R. Kuniyoshi, A. Taniyama, M. Yokoyama, S. Sakajiri, K. Takeuchi, C. Watanabe, S. Takahashi, Y. Ito, K. Hatake, Identification of CD20 C-terminal deletion mutations associated with loss of CD20 expression in non-Hodgkin's lymphoma, Clin. Cancer Res. 15 (2009) 2523–2530.
[14] R. Lapalombella, B. Yu, G. Triantafillou, Q. Liu, J.P. Butchar, G. Lozanski, A. Ramanunni, L.L. Smith, W. Blum, L. Andritsos, D.S. Wang, A. Lehman, C.S. Chen, A.J. Johnson, G. Marcucci, R.J. Lee, L.J. Lee, S. Tridandapani, N. Muthusamy, J.C. Byrd, Lenalidomide down-regulates the CD20 antigen and antagonizes direct and antibody-dependent cellular cytotoxicity of rituximab on primary chronic lymphocytic leukemia cells, Blood (2008).

[15] A.R. Jazirehi, M.I. Vega, B. Bonavida, Development of rituximab-resistant lymphoma clones with altered cell signaling and cross-resistance to chemotherapy, Cancer Res. 67 (2007) 1270–1281.
[16] B. Bonavida, Rituximab-induced inhibition of antiapoptotic cell survival pathways: implications in chemo/immunoresistance, rituximab unresponsiveness, prognostic and novel therapeutic interventions, Oncogene 26 (2007) 3629–3636.
[17] T. van Meerten, R.S. van Rijn, S. Hol, A. Hagenbeek, S.B. Ebeling, Complement-induced cell death by rituximab depends on CD20 expression level and acts complementary to antibody-dependent cellular cytotoxicity, Clin. Cancer Res. 12 (2006) 4027–4035.
[18] N.A. Johnson, M. Boyle, A. Bashashati, S. Leach, A. Brooks-Wilson, L.H. Sehn, M. Chhanabhai, R.R. Brinkman, J.M. Connors, A.P. Weng, R.D. Gascoyne, Diffuse large B-cell lymphoma: reduced CD20 expression is associated with an inferior survival, Blood 113 (2009) 3773–3780.
[19] G. Egger, G. Liang, A. Aparicio, P.A. Jones, Epigenetics in human disease and prospects for epigenetic therapy, Nature 429 (2004) 457–463.
[20] C.B. Yoo, P.A. Jones, Epigenetic therapy of cancer: past, present and future, Nat. Rev. Drug Discov. 5 (2006) 37–50.
[21] A. Tomita, D.R. Buchholz, Y.B. Shi, Recruitment of N-CoR/SMRT-TBLR1 corepressor complex by unliganded thyroid hormone receptor for gene repression during frog development, Mol. Cell. Biol. 24 (2004) 3337–3346.
[22] A. Atsumi, A. Tomita, H. Kiyoi, T. Naoe, Histone deacetylase 3 (HDAC3) is recruited to target promoters by PML-RARalpha as a component of the N-CoR co-repressor complex to repress transcription in vivo, Biochem. Biophys. Res. Commun. 345 (2006) 1471–1480.
[23] A. Tomita, D.R. Buchholz, K. Obata, Y.B. Shi, Fusion protein of retinoic acid receptor alpha with promyelocytic leukemia protein or promyelocytic leukemia zinc finger protein recruits N-CoR-TBLR1 corepressor complex to repress transcription in vivo, J. Biol. Chem. 278 (2003) 30788–30795.
[24] K. Ghoshal, J. Datta, S. Majumder, S. Bai, H. Kutay, T. Motiwala, S.T. Jacob, 5-Aza-deoxycytidine induces selective degradation of DNA methyltransferase 1 by a proteasomal pathway that requires the KEN box, bromo-adjacent homology domain, and nuclear localization signal, Mol. Cell. Biol. 25 (2005) 4727–4741.
[25] A. Himmelmann, A. Riva, G.L. Wilson, B.P. Lucas, C. Thevenin, J.H. Kehrl, PU.1/Pip and basic helix loop helix zipper transcription factors interact with binding sites in the CD20 promoter to help confer lineage- and stage-specific expression of CD20 in B lymphocytes, Blood 90 (1997) 3984–3995.
[26] M.G. Rosenfeld, V.V. Lunyak, C.K. Glass, Sensors and signals: a coactivator/corepressor/epigenetic code for integrating signal-dependent programs of transcriptional response, Genes Dev. 20 (2006) 1405–1428.
[27] S.A. Denslow, P.A. Wade, The human Mi-2/NuRD complex and gene regulation, Oncogene 26 (2007) 5433–5438.
[28] J. Li, J. Wang, Z. Nawaz, J.M. Liu, J. Qin, J. Wong, Both corepressor proteins SMRT and N-CoR exist in large protein complexes containing HDAC3, EMBO J. 19 (2000) 4342–4350.
[29] A. Hagenbeek, O. Gadeberg, P. Johnson, L.M. Pedersen, J. Walewski, A. Hellmann, B.K. Link, T. Robak, M. Wojtukiewicz, M. Pfreundschuh, M. Kneba, A. Engert, P. Sonneveld, M. Flensburg, J. Petersen, N. Losic, J. Radford, First clinical use of ofatumumab, a novel fully human anti-CD20 monoclonal antibody in relapsed or refractory follicular lymphoma: results of a phase 1/2 trial, Blood 111 (2008) 5486–5495.
[30] T. Robak, GA-101, a third-generation, humanized and glyco-engineered anti-CD20 mAb for the treatment of B-cell lymphoid malignancies, Curr. Opin. Investig. Drugs 10 (2009) 588–596.

Down-regulation of CD20 expression in B-cell lymphoma cells after treatment with rituximab-containing combination chemotherapies: its prevalence and clinical significance

Junji Hiraga,[1,2] Akihiro Tomita,[1] Takumi Sugimoto,[1] Kazuyuki Shimada,[1] Masafumi Ito,[3] Shigeo Nakamura,[4] Hitoshi Kiyoi,[5] Tomohiro Kinoshita,[1] and Tomoki Naoe[1]

[1]Department of Hematology and Oncology, Nagoya University Graduate School of Medicine, Nagoya; [2]Department of Hematology, Toyota Memorial Hospital, Toyota; [3]Department of Pathology, Japanese Red Cross, Nagoya First Hospital, Nagoya; [4]Department of Pathology and Clinical Laboratories, Nagoya University Hospital, Nagoya; and [5]Department of Infectious Diseases, Nagoya University School of Medicine, Nagoya, Japan

Although rituximab is a key molecular targeting drug for CD20-positive B-cell lymphomas, resistance to rituximab has recently been recognized as a considerable problem. Here, we report that a CD20-negative phenotypic change after chemotherapies with rituximab occurs in a certain number of CD20-positive B-cell lymphoma patients. For 5 years, 124 patients with B-cell malignancies were treated with rituximab-containing chemotherapies in Nagoya University Hospital. Relapse or progression was confirmed in 36 patients (29.0%), and a rebiopsy was performed in 19 patients. Of those 19, 5 (26.3%; diffuse large B-cell lymphoma [DLBCL], 3 cases; DLBCL transformed from follicular lymphoma, 2 cases) indicated CD20 protein-negative transformation. Despite salvage chemotherapies without rituximab, all 5 patients died within 1 year of the CD20-negative transformation. Quantitative reverse-transcription–polymerase chain reaction (RT-PCR) showed that CD20 mRNA expression was significantly lower in CD20-negative cells than in CD20-positive cells obtained from the same patient. Interestingly, when CD20-negative cells were treated with 5-aza-2′-deoxycytidine in vitro, the expression of CD20 mRNA was stimulated within 3 days, resulting in the restoration of both cell surface expression of the CD20 protein and rituximab sensitivity. These findings suggest that some epigenetic mechanisms may be partly related to the down-regulation of CD20 expression after rituximab treatment. (Blood. 2009;113: 4885-4893)

Introduction

Rituximab is a murine/human chimeric anti-CD20 monoclonal antibody that has become a key molecular targeting drug for CD20-positive B-cell lymphomas.[1,2] Many favorable results using combination chemotherapy with rituximab for both CD20-positive de novo and relapsed low-grade and aggressive B-cell non-Hodgkin lymphoma have been reported in recent years.[3-7] In Japan, rituximab has also been used since September 2001 for patients with follicular lymphoma (FL), indolent lymphoma, and mantle cell lymphoma (MCL). In addition, since September 2003 in Japan, indications for using rituximab were expanded to include diffuse large B-cell lymphoma (DLBCL), further demonstrating the significant effectiveness of rituximab for B-cell lymphoma compared with conventional chemotherapies without rituximab.[8]

Although combination chemotherapies with rituximab have provided significantly favorable results for CD20-positive B-cell lymphoma patients, acquired resistance to rituximab has become a considerable problem. Several mechanisms of resistance were predicted as reported previously, including loss of CD20 expression, inhibition of antibody binding, antibody metabolism, expression of complement inhibitors such as CD55/CD59, and membrane/lipid raft abnormality (reviewed by Smith et al[9]),[10-19] but the clinical significance of those mechanisms has remained unclear. In the last 5 years, a CD20-negative phenotypic change in CD20-positive lymphomas after rituximab treatment has been reported by several groups,[16,20-31] indicating that this phenomenon after the use of rituximab may not be rare. Although these reports contain important information from clinical experiences, the frequency of occurrence and detailed molecular biologic information about the CD20-negative phenotype remain to be elucidated.

Very recently, we reported a CD20-negative DLBCL case that had transformed from CD20-positive FL after repeated treatment with rituximab. We established an RRBL1 cell line from this patient,[32] and the mechanisms of the CD20-negative change were analyzed in these cells. CD20 mRNA expression was significantly lower than in CD20-positive cells, resulting in a loss of CD20 protein expression as detected by flow cytometry (FCM), immunohistochemistry (IHC), and immunoblotting (IB). Interestingly, trichostatin A (TSA), a histone deacetylase inhibitor, was able to successfully stimulate CD20 expression, suggesting that some epigenetic mechanisms may have repressed the expression. Thus, an accumulation of detailed clinical and molecular biologic features is required to demonstrate the significance of CD20-negative phenotypic changes after rituximab treatment.

In the last 5 years, 124 patients with CD20-positive B-cell malignancies received chemotherapy with rituximab at Nagoya University Hospital, 36 (29.0%) of whom showed relapse/progression. Among these 36 patients, CD20 protein-negative or -decreased phenotypic changes were confirmed in 5 cases concomitant with disease progression. Here, we describe the occurrence rate of CD20-negative transformation after rituximab treatment, as well

Submitted August 19, 2008; accepted February 25, 2009. Prepublished online as *Blood* First Edition paper, February 26, 2009; DOI 10.1182/blood-2008-08-175208.

The online version of this article contains a data supplement.

The publication costs of this article were defrayed in part by page charge payment. Therefore, and solely to indicate this fact, this article is hereby marked "advertisement" in accordance with 18 USC section 1734.